

000 001 002 003 004 005 006 007 008 009 010 011 012 013 014 015 016 017 018 019 020 021 022 023 024 025 026 027 028 029 030 031 032 033 034 035 036 037 038 039 040 041 042 043 044 045 046 047 048 049 050 051 052 053 IMPROVED ANALYSIS FOR SIGN-BASED METHODS WITH MOMENTUM UPDATES

Anonymous authors

Paper under double-blind review

ABSTRACT

This paper presents enhanced analysis for sign-based optimization algorithms with momentum updates. Traditional sign-based methods obtain a convergence rate of $\mathcal{O}(T^{-1/4})$ under the separable smoothness assumption, but they typically require large batch sizes or assume unimodal symmetric stochastic noise. To address these limitations, we demonstrate that signSGD with momentum can achieve the same convergence rate using constant batch sizes without additional assumptions. We also establish a convergence rate under the l_2 -smoothness condition, improving upon the result of the prior momentum-based signSGD variant by a factor of $\mathcal{O}(d^{1/2})$, where d is the problem dimension. Furthermore, we explore sign-based methods with majority vote in distributed settings and show that the proposed momentum-based method yields convergence rates of $\mathcal{O}(d^{1/2}T^{-1/2} + dn^{-1/2})$ and $\mathcal{O}(\max\{d^{1/4}T^{-1/4}, d^{1/10}T^{-1/5}\})$, which outperform the previous results of $\mathcal{O}(dT^{-1/4} + dn^{-1/2})$ and $\mathcal{O}(d^{3/8}T^{-1/8})$, respectively. Numerical experiments also validate the effectiveness of the proposed methods.

1 INTRODUCTION

This paper investigates the stochastic optimization problem in the form

$$\min_{\mathbf{x} \in \mathbb{R}^d} f(\mathbf{x}), \quad (1)$$

where $f : \mathbb{R}^d \rightarrow \mathbb{R}$ is a smooth function. We assume that only noisy estimations of the gradient are available, denoted as $\nabla f(\mathbf{x}; \xi)$, where ξ is a random sample such that $\mathbb{E}[\nabla f(\mathbf{x}; \xi)] = \nabla f(\mathbf{x})$.

Problem (1) has been extensively studied in the literature (Duchi et al., 2011; Kingma & Ba, 2015; Loshchilov & Hutter, 2017; Fang et al., 2018; Wang et al., 2019). One of the most widely used methods for this problem is Stochastic Gradient Descent (SGD), which updates the parameters as:

$$\mathbf{x}_{t+1} = \mathbf{x}_t - \eta \nabla f(\mathbf{x}_t; \xi_t), \quad (2)$$

where η is the learning rate and ξ_t is the random sample drawn at the t -th iteration. It is known that SGD achieves a convergence rate of $\mathcal{O}(T^{-1/4})$, where T is the number of iterations (Ghadimi & Lan, 2013). This rate is proved to be optimal under standard assumptions (Arjevani et al., 2023).

Instead of using the stochastic gradient to update, several works (Bernstein et al., 2018; 2019; Safaryan & Richtarik, 2021) propose to update using only the sign of the stochastic gradient, i.e.,

$$\mathbf{x}_{t+1} = \mathbf{x}_t - \eta \text{sign}(\nabla f(\mathbf{x}_t; \xi_t)), \quad (3)$$

which is particularly beneficial in distributed settings. In such scenarios, only the sign information needs to be transmitted between nodes, significantly reducing communication overhead.

Recently, several studies have investigated the convergence properties of signSGD and its variants. Bernstein et al. (2018) first prove that signSGD achieves a convergence rate of $\mathcal{O}(N^{-1/4})$ under the separable smoothness assumption, where N is the number of stochastic gradient calls. However, their analysis requires a large batch size of $\mathcal{O}(\sqrt{N})$ in each iteration. Later, Bernstein et al. (2019) demonstrate that signSGD can achieve the same convergence rate with constant batch sizes, but under the additional assumption that the noise is unimodal and symmetric. To avoid such extra

054
 055 Table 1: Summary of convergence rates for sign-based algorithms. Here, T represents the number of
 056 stochastic gradient calls and $l_1 \& l_2$ denotes mixed l_1 -norm and weighted l_2 -norm. We use stochastic
 057 gradient calls rather than iteration numbers to measure convergence, in order to provide a fairer
 058 comparison across different algorithms with varying batch sizes.

Method	Convergence	Assumptions	Measure	Additional Requirements
signSGD (Bernstein et al., 2018)	$\mathcal{O}\left(\frac{1}{T^{1/4}}\right)$		l_1	Large batch size of $\mathcal{O}(\sqrt{T})$
Signum (Bernstein et al., 2018)	$\tilde{\mathcal{O}}\left(\frac{1}{T^{1/4}}\right)$		l_1	Large batch size of $\mathcal{O}(\sqrt{T})$
signSGD (Bernstein et al., 2019)	$\mathcal{O}\left(\frac{1}{T^{1/4}}\right)$	Assumptions 1, 2, 3	$l_1 \& l_2$	Unimodal symmetric noise
Theorem 1 (this work)	$\mathcal{O}\left(\frac{1}{T^{1/4}}\right)$		l_1	—
signSGD-SIM (Sun et al., 2023)	$\mathcal{O}\left(\frac{d}{T^{1/4}}\right)$			
Theorem 2 (this work)	$\mathcal{O}\left(\frac{d^{1/2}}{T^{1/4}}\right)$	Assumptions 1, 4, 5	l_1	—

069 assumptions, Sun et al. (2023) show that signSGD with momentum can achieve a convergence rate of
 070 $\mathcal{O}(dT^{-1/4})$ under the l_2 -smoothness assumption. However, this dependence on d is unsatisfactory,
 071 leading to high sample complexity for high-dimensional problems.

072 In this paper, we re-examine signSGD with momentum and establish a convergence rate of
 073 $\mathcal{O}(T^{-1/4})$ under the separable smoothness condition. Compared with previous work (Bernstein
 074 et al., 2018; 2019), our analysis does not require large batch sizes or unimodal symmetric noise. Un-
 075 der the l_2 -smoothness assumption, we also derive a convergence rate of $\mathcal{O}(d^{1/2}T^{-1/4})$, improving
 076 the previous result of $\mathcal{O}(dT^{-1/4})$ (Sun et al., 2023).

077 For distributed sign-based methods, each node typically transmits the sign of its gradient to the
 078 server, which then sends back the sign of the aggregated gradients for update. In this context, previ-
 079 ous literature establishes convergence rates of $\mathcal{O}\left(\frac{d}{T^{1/4}} + \frac{d}{n^{1/2}}\right)$ (Sun et al., 2023) and $\mathcal{O}\left(\frac{d^{3/8}}{T^{1/8}}\right)$ (Jin
 080 et al., 2021), where n denotes the number of nodes. To improve these rates, we utilize an unbiased
 081 sign operation along with momentum updates, achieving convergence rates of $\mathcal{O}\left(\frac{d^{1/2}}{T^{1/2}} + \frac{d}{n^{1/2}}\right)$,
 082 $\mathcal{O}\left(\frac{n^{1/2}}{T} + \frac{d}{n^{1/2}}\right)$ and $\mathcal{O}\left(\max\left\{\frac{d^{1/4}}{T^{1/4}}, \frac{d^{1/10}}{T^{1/5}}\right\}\right)$, with different hyper-parameter settings and algo-
 083 rithm designs. In summary, this paper makes the following contributions:

- 084 • Under the separable smoothness assumption, we prove that signSGD with momentum can
 085 achieve a convergence rate of $\mathcal{O}(T^{-1/4})$ without additional assumptions. In contrast, ex-
 086 isting analyses require either large batches or the assumption of unimodal symmetric noise.
- 087 • Under the l_2 -smoothness assumption, we show that signSGD with momentum achieves a
 088 convergence rate of $\mathcal{O}(d^{1/2}T^{-1/4})$, improving upon the $\mathcal{O}(dT^{-1/4})$ result of the existing
 089 momentum-based signSGD method under the same conditions.
- 090 • In distributed settings, we derive convergence rates of $\mathcal{O}\left(\frac{n^{1/2}}{T} + \frac{d}{n^{1/2}}\right)$, $\mathcal{O}\left(\frac{d^{1/2}}{T^{1/2}} + \frac{d}{n^{1/2}}\right)$
 091 and $\mathcal{O}\left(\max\left\{\frac{d^{1/4}}{T^{1/4}}, \frac{d^{1/10}}{T^{1/5}}\right\}\right)$, with the latter two substantially outperforming previous re-
 092 sults of $\mathcal{O}\left(\frac{d}{T^{1/4}} + \frac{d}{n^{1/2}}\right)$ and $\mathcal{O}\left(\frac{d^{3/8}}{T^{1/8}}\right)$, respectively.

107 We compare our results with existing methods in Tables 1 and 2.

108
109
110
111 Table 2: Summary of results for sign-based algorithms in the distributed setting, where n represents
112 the number of nodes and T denotes the iteration number.
113
114
115
116
117
118

Method	Convergence	Measure
MV-sto-signSGD-SIM (Sun et al., 2023)	$\mathcal{O}\left(\frac{d}{T^{1/4}} + \frac{d}{n^{1/2}}\right)$	
Theorem 3 (this work)	$\mathcal{O}\left(\frac{d^{1/2}}{T^{1/2}} + \frac{d}{n^{1/2}}\right)$	l_1
Theorem 4 (this work)	$\mathcal{O}\left(\frac{n^{1/2}}{T} + \frac{d}{n^{1/2}}\right)$	
Sto-signSGD (Jin et al., 2021)	$\mathcal{O}\left(\frac{d^{3/8}}{T^{1/8}}\right)$	
Theorem 5 (this work)	$\mathcal{O}\left(\max\left\{\frac{d^{1/4}}{T^{1/4}}, \frac{d^{1/10}}{T^{1/5}}\right\}\right)$	l_2

123
124
125

2 RELATED WORK

126
127 In this section, we review the signSGD method and its variants, as well as sign-based methods with
128 majority vote in distributed settings.129
130

2.1 SIGNSGD AND ITS VARIANTS

131
132 The convergence of signSGD is first analyzed by Bernstein et al. (2018), who obtain a rate of
133 $\mathcal{O}(N^{-1/4})$ with a large batch size of $\mathcal{O}(\sqrt{N})$, where N is the number of stochastic gradient calls.
134 They also show that the momentum version of signSGD, named Signum, achieves a convergence
135 rate of $\mathcal{O}(N^{-1/4} \log N)$ with increasingly large batches. To avoid large batch sizes, Bernstein et al.
136 (2019) attain the same convergence rate with a constant batch size, but rely on the strong assumption
137 that the stochastic gradient noise is both unimodal and symmetric, which is not satisfied for many
138 types of noise in practice.139 Subsequently, Karimireddy et al. (2019) observe that signSGD with a constant batch size may not
140 converge to optimal points for convex objectives and performs poorly compared to traditional SGD.
141 To address this, they incorporate the compression error into the next update step and show that error
142 feedback enhances practical performance. **However, their error-feedback method needs to transmit**
143 **additional information and further assumes the bounded gradient assumption, making their analyses**
144 **non-standard.** Rather than assuming unbiased estimation and bounded noise, Safaryan & Richtarik
145 (2021) provide convergence guarantees under the success probability bounds assumption, which
146 posits that the sign of the stochastic gradient matches that of the true gradient with a probability
147 greater than 1/2. Recently, Sun et al. (2023) analyze the momentum-based version of signSGD and
148 achieve a convergence rate of $\mathcal{O}(dT^{-1/4})$ under standard assumptions. However, their dependence
149 on d can be further improved, as demonstrated by our analysis.150 Besides, several other variants have been proposed. For instance, ZO-signSGD (Liu et al., 2019)
151 combines zeroth-order updates with sign information, ensuring gradient-free and communication
152 compression. Jiang et al. (2024) incorporate variance reduction with sign operation, improving the
153 convergence to $\mathcal{O}(T^{-1/3})$ under a stronger smoothness assumption and to $\mathcal{O}(d^{1/2}m^{1/4}T^{-1/2})$ for
154 finite-sum problems, where m denotes the number of functions in the finite-sum structure. **However,**
155 **their $\mathcal{O}(T^{-1/3})$ result is obtained under the stronger average smoothness assumption, which requires**
156 **that each stochastic sample is smooth. Additionally, their proposed method involves computing the**
157 **gradient at the previous decision point, resulting in additional computational overhead.**158
159

2.2 SIGN-BASED METHODS WITH MAJORITY VOTE

160 The majority vote technique is employed to enable communication compression in distributed set-
161 tings. In this framework, each node transmits only the sign of its gradient estimation to the pa-
rameter server, which then aggregates the information and sends the sign of the aggregated data

back to each node for updating. In the homogeneous setting, Bernstein et al. (2018) first demonstrate that signSGD with majority vote can achieve a convergence rate of $\mathcal{O}(T^{-1/4})$ with large batch sizes. Later, Bernstein et al. (2019) further obtain the same rate with a constant batch size when the noise is unimodal and symmetric. For more challenging heterogeneous environments, the SSDM method (Safaryan & Richtarik, 2021) achieves a convergence rate of $\mathcal{O}(d^{1/2}T^{-1/4})$ under the success probability bounds assumption. However, SSDM only guarantees 1-bit compression in one direction, since the information sent back to each node is not the sign information anymore. To address this, Stochastic-Sign SGD (Jin et al., 2021) ensures 1-bit compression in both directions and achieves a convergence rate of $\mathcal{O}(d^{3/8}T^{-1/8})$ in terms of the l_2 -norm. Later, Sun et al. (2023) propose the MV-sto-signSGD-SIM method, attaining a convergence rate of $\mathcal{O}(\frac{d}{T^{1/4}} + \frac{d}{n^{1/2}})$. By incorporating variance reduction techniques, Jiang et al. (2024) improve the convergence rates to $\mathcal{O}(\frac{d^{1/2}}{T^{1/2}} + \frac{d}{n^{1/2}})$ and $\mathcal{O}(d^{1/4}T^{-1/4})$, under a stronger average smoothness assumption.

3 SIGNSGD WITH MOMENTUM UPDATES

In this section, we first introduce the assumptions used to analyze sign-based methods and then present our convergence guarantees for signSGD with momentum. Due to space limitations, all proofs are deferred to the Appendix.

3.1 ASSUMPTIONS

We outline the assumptions commonly used to derive convergence guarantees for sign-based methods (Bernstein et al., 2018; 2019).

Assumption 1 $f_* = \inf_x f(x) > -\infty$ and $f(\mathbf{x}_1) - f_* \leq \Delta_f$ for the initial solution \mathbf{x}_1 .

Assumption 2 (Separable smoothness) The objective function f is separable smooth if there exist non-negative constants $[L_1, L_2, \dots, L_d]$ such that

$$f(\mathbf{y}) \leq f(\mathbf{x}) + \langle \nabla f(\mathbf{x}), \mathbf{y} - \mathbf{x} \rangle + \frac{1}{2} \sum_{i=1}^d L_i (\mathbf{y}_i - \mathbf{x}_i)^2.$$

Assumption 3 (Separable bounded noise) For non-negative constants $[\sigma_1, \sigma_2, \dots, \sigma_d]$, we have

$$\mathbb{E}_\xi \left[(\nabla f(\mathbf{x}; \xi))_i - [\nabla f(\mathbf{x})]_i \right]^2 \leq \sigma_i^2.$$

Instead of using Assumptions 2 and 3, other literature (Sun et al., 2023; Jiang et al., 2024) employs the following assumptions alternatively.

Assumption 4 (l_2 -smoothness) The objective function f is L -smooth if

$$\|\nabla f(\mathbf{x}) - \nabla f(\mathbf{y})\| \leq L \|\mathbf{x} - \mathbf{y}\|.$$

Assumption 5 (Bounded noise) The stochastic gradient noise is bounded such that

$$\mathbb{E}_\xi \left[\|\nabla f(\mathbf{x}; \xi) - \nabla f(\mathbf{x})\|^2 \right] \leq \sigma^2.$$

Remark: To align with different literature, we provide two distinct theorems in the next subsection, derived under Assumptions 1, 2, 3 and Assumptions 1, 4, 5 respectively.

3.2 THE CONVERGENCE GUARANTEES

Here, we introduce the sign-based method with momentum updates and present the corresponding convergence guarantees. The traditional signSGD method uses the sign of the stochastic gradient for updates, in the form of equation (3). In contrast to the signSGD method, we track the gradient using a momentum estimator \mathbf{v}_t , defined as

$$\mathbf{v}_t = (1 - \beta)\mathbf{v}_{t-1} + \beta \nabla f(\mathbf{x}_t; \xi_t), \quad (4)$$

216 **Algorithm 1** Signum

```

217 1: Input: iteration number  $T$ , initial point  $\mathbf{x}_1$ 
218 2: for time step  $t = 1$  to  $T$  do
219 3:   if  $t == 1$  then
220 4:     Compute  $\mathbf{v}_t = \nabla f(\mathbf{x}_t; \xi_t)$ 
221 5:   else
222 6:     Compute  $\mathbf{v}_t = (1 - \beta)\mathbf{v}_{t-1} + \beta \nabla f(\mathbf{x}_t; \xi_t)$ 
223 7:   end if
224 8:   Update the decision variable:  $\mathbf{x}_{t+1} = \mathbf{x}_t - \eta \text{sign}(\mathbf{v}_t)$ 
225 9: end for
226 10: Select  $\tau$  uniformly at random from  $\{1, \dots, T\}$ 
227 11: Return  $\mathbf{x}_\tau$ 
228
229
```

230 where β is the momentum parameter and we use $\mathbf{v}_1 = \nabla f(\mathbf{x}_1; \xi_1)$ for the first iteration. After
231 computing the estimator \mathbf{v}_t , we update the decision variable using the sign of \mathbf{v}_t as follows:

$$232 \quad \mathbf{x}_{t+1} = \mathbf{x}_t - \eta \text{sign}(\mathbf{v}_t). \quad (5)$$

233 The full algorithm is outlined in Algorithm 1, which is called Signum in the previous work (Bern-
234 stein et al., 2018) (also named as signSGD-SIM by Sun et al. (2023)). Our contribution lies in the
235 improved theoretical analysis. To compare with previous signSGD studies (Bernstein et al., 2018;
236 2019), we first provide guarantees under the separable smoothness assumption.

237 **Theorem 1** *Under Assumptions 1, 2 and 3, by setting $\beta = \mathcal{O}(T^{-1/2})$ and $\eta = \mathcal{O}(T^{-3/4})$, Algo-
238 rithm 1 ensures that*

$$239 \quad \mathbb{E}[\|\nabla f(\mathbf{x}_\tau)\|_1] \leq \mathcal{O}\left(\frac{1}{T^{1/4}}\right).$$

240 **Remark:** The above rate implies a sample complexity of $\mathcal{O}(\epsilon^{-4})$, matching the state-of-the-art
241 results for signSGD (Bernstein et al., 2018; 2019). However, our method does not require large
242 batch sizes which can be as large as $\mathcal{O}(\epsilon^{-2})$ for signSGD (Bernstein et al., 2018), and avoids the
243 unimodal symmetric noise assumption required by Bernstein et al. (2019).

244 Next, we also provide the theoretical guarantee under the l_2 -smoothness assumption.

245 **Theorem 2** *Under Assumptions 1, 4 and 5, by setting $\beta = \mathcal{O}(T^{-1/2})$ and $\eta = \mathcal{O}(d^{-1/2}T^{-3/4})$,
246 Algorithm 1 ensures that*

$$247 \quad \mathbb{E}[\|\nabla f(\mathbf{x}_\tau)\|_1] \leq \mathcal{O}\left(\frac{d^{1/2}}{T^{1/4}}\right).$$

248 **Remark:** This rate implies a sample complexity of $\mathcal{O}(d^2\epsilon^{-4})$, an improvement over the $\mathcal{O}(d^4\epsilon^{-4})$
249 results of previous sign-based momentum methods (Sun et al., 2023). This improvement is espe-
250 cially significant when the dimension d is large.

251 **Remark:** In Theorem 1, by using the separable smoothness and separable bounded noise assump-
252 tions (Assumptions 2 and 3), we can directly analyze under the ℓ_1 -norm and provide coordinate-wise
253 bounds, thus avoiding the $d^{1/2}$ dependency.

254 **Source of Theoretical Improvement:** In the previous work (Bernstein et al., 2018), to bound
255 the term $\sum_i |[\nabla f(\mathbf{x}_t)]_i| \cdot \mathbb{P}(\text{sign}([\nabla f(\mathbf{x}_t)]_i) \neq \text{sign}([\mathbf{v}_t]_i))$ appeared in the analysis, they apply
256 $\mathbb{P}(\text{sign}([\nabla f(\mathbf{x}_t)]_i) \neq \text{sign}(\nabla f(\mathbf{x}_t; \xi_t)_i)) \leq \frac{\sigma_i}{\sqrt{n_i} |[\nabla f(\mathbf{x}_t)]_i|}$, which inevitably requires *huge batch*
257 *sizes* n_i to ensure convergence. Later work (Bernstein et al., 2019) assumes *unimodal symmetric*
258 *noise* to deal with $\mathbb{P}(\text{sign}([\nabla f(\mathbf{x}_t)]_i) \neq \text{sign}([\mathbf{v}_t]_i))$. While in our analysis, we find that standard
259 assumption is already adequate and we use $\sum_i |[\nabla f(\mathbf{x}_t)]_i| \cdot \mathbb{P}(\text{sign}([\nabla f(\mathbf{x}_t)]_i) \neq \text{sign}([\mathbf{v}_t]_i)) \leq$
260 $\sum_i |[\nabla f(\mathbf{x}_t)]_i - [\mathbf{v}_t]_i| \leq \|\nabla f(\mathbf{x}_t) - \mathbf{v}_t\|_1$ in the analysis. Since we further provide a tighter bound
261 for the estimation error $\|\nabla f(\mathbf{x}_t) - \mathbf{v}_t\|_1$ compared to Sun et al. (2023), we achieve the state-of-the-
262 art convergence rate without relying on additional assumptions.

270 3.3 SHARPNESS OF THE OBTAINED RATES
271272 The convergence lower bound for stochastic optimization is $\Omega(T^{-1/4})$ in the l_2 -norm (Arjevani
273 et al., 2023). Since we know that $\|z\|_1 \geq \|z\|_2$, this lower bound also implies that $\mathbb{E}[\|\nabla f(\mathbf{x}_\tau)\|_1] \geq$
274 $\mathbb{E}[\|\nabla f(\mathbf{x}_\tau)\|_2] \geq \Omega(T^{-1/4})$, indicating that our result is optimal with respect to T .275 Regarding the $d^{1/2}$ factor in the convergence rate, several pieces of evidence suggest that this factor
276 is inherent for l_1 -norm convergence under the standard l_2 -smoothness assumption:
277278 • Jiang et al. (2025) establish an $\Omega\left(\sqrt{\frac{d\|L\|_\infty}{T}} + \frac{d^{1/4}(\sum_{i=1}^d \sigma_i \sqrt{L_i})^{1/2}}{T^{1/4}}\right)$ lower bound for SGD
279 when measured with the l_1 -norm. Suppose that $\{\sigma_i\}$ and $\{L_i\}$ have the same value across co-
280 ordinates such that $\sigma_i = \sigma/\sqrt{d}$, $L_i = L$, the lower bound becomes $\Omega\left(\frac{d^{1/2}}{T^{1/4}}\right)$, which confirms
281 the \sqrt{d} factor is required in the l_1 -norm setting.
282 • Prior works (Bernstein et al., 2018; Dong et al., 2024) have already conducted extensive ex-
283 periments on various vision and language tasks, and find that the ratio of the gradient norm
284 $r = \|\nabla f(\mathbf{x})\|_1 / \|\nabla f(\mathbf{x})\|_2$ always stay close to the level of $\Theta(\sqrt{d})$, supporting the presence
285 of the \sqrt{d} factor in the l_1 measure from the empirical sense.
286 • Existing rates for sign-based methods under the l_1 -norm and l_2 -smoothness assumption also
287 include the \sqrt{d} dependency, or even worse (Jin et al., 2021; Sun et al., 2023). Our Theorem 2
288 already improves the d -dependency from Sun et al. (2023) under the same assumptions.
289290 4 MAJORITY VOTE SIGNSGD WITH MOMENTUM UPDATES
291292 We first present the problem formulation and the assumptions used. Then, we introduce the proposed
293 method and establish the convergence guarantees.
294295 4.1 PROBLEM FORMULATION AND ASSUMPTIONS
296297 Sign-based methods are highly communication-efficient in distributed settings, as they only require
298 1-bit sign information for updates. Previous literature (Bernstein et al., 2018; 2019; Jin et al., 2021;
299 Sun et al., 2023) has analyzed sign-based methods with majority vote in distributed environments.
300 To begin with, consider the following distributed learning problem:
301

302
$$\min_{\mathbf{x} \in \mathbb{R}^d} f(\mathbf{x}) := \frac{1}{n} \sum_{j=1}^n f_j(\mathbf{x}), \quad f_j(\mathbf{x}) = \mathbb{E}_{\xi^j \sim \mathcal{D}_j} [f_j(\mathbf{x}; \xi^j)], \quad (6)$$

303

304 where \mathcal{D}_j represents the data distribution on node j , and $f_j(\mathbf{x})$ is the corresponding loss function.
305306 Early studies (Bernstein et al., 2018; 2019) focus on homogeneous settings, where \mathcal{D}_j and f_j are
307 identical across nodes. For the more difficult heterogeneous setting, Jin et al. (2021) derive a conver-
308 gence rate of $\mathcal{O}(d^{3/8}T^{-1/8})$ and Sun et al. (2023) achieve the rate of $\mathcal{O}(\frac{d}{T^{1/4}} + \frac{d}{n^{1/2}})$. However,
309 these rates can still be improved based on our analysis.
310311 Next, we introduce the assumptions required in this section, which are standard and commonly used
312 in previous works (Jin et al., 2021; Sun et al., 2023).
313314 **Assumption 6** (Smoothness on node j) For each node $j \in [n]$, we suppose
315

316
$$\|\nabla f_j(\mathbf{x}) - \nabla f_j(\mathbf{y})\| \leq L \|\mathbf{x} - \mathbf{y}\|.$$

317 **Assumption 7** (Bounded noise on node j) For each node $j \in [n]$, we have
318

319
$$\mathbb{E}_\xi [\|\nabla f_j(\mathbf{x}; \xi) - \nabla f_j(\mathbf{x})\|^2] \leq \sigma^2.$$

320 **Assumption 8** (Bounded gradients) For each node $j \in [n]$, we assume $\sup_{\mathbf{x}} \|\nabla f_j(\mathbf{x}; \xi)\|_\infty \leq G$.
321322 **Remark:** The bounded gradients assumption is standard and widely employed for sign-based op-
323 timization in heterogeneous settings (Jin et al., 2021; Sun et al., 2023; Tang et al., 2024). Also
324 note that our Assumption 8 is strictly weaker than the one used by Sun et al. (2023), which requires
325 bounded gradients in the l_2 -norm, i.e., $\sup_{\mathbf{x}} \|\nabla f_j(\mathbf{x}; \xi)\|_2 \leq G$.
326

324 4.2 THE PROPOSED METHOD
325

326 In this subsection, we introduce the proposed method for the heterogeneous distributed environments
327 and aim to obtain improved convergence rates without additional strong assumptions. For distributed
328 settings, the most straightforward approach is to apply the sign operation twice:

$$329 \quad 330 \quad 331 \quad 332 \quad \mathbf{x}_{t+1} = \mathbf{x}_t - \eta \operatorname{sign} \left(\frac{1}{n} \sum_{j=1}^n \operatorname{sign}(\mathbf{v}_t^j) \right), \quad (7)$$

333 where \mathbf{v}_t^j is the gradient estimator at node j . In this formulation, each node transmits the sign of its
334 gradient estimate $\operatorname{sign}(\mathbf{v}_t^j)$ to the server. The server then aggregates these sign values and broadcasts
335 back the sign of the resulting information $\operatorname{sign} \left(\frac{1}{n} \sum_{j=1}^n \operatorname{sign}(\mathbf{v}_t^j) \right)$ to each node for updating. This
336 approach ensures 1-bit communication in both directions. However, the sign operation introduces
337 bias in the estimation, and applying it twice can significantly amplify this bias. To mitigate this, we
338 introduce an unbiased sign operation (Sun et al., 2023) as stated below.

340 **Definition 1** For any vector \mathbf{v} with $\|\mathbf{v}\|_\infty \leq R$, the function $S_R(\mathbf{v})$ is defined component-wise by:
341

$$342 \quad 343 \quad 344 \quad 345 \quad [S_R(\mathbf{v})]_k = \begin{cases} 1, & \text{with probability } \frac{R+[\mathbf{v}]_k}{2R}, \\ -1, & \text{with probability } \frac{R-[\mathbf{v}]_k}{2R}. \end{cases} \quad (8)$$

346 **Remark:** This operation provides an unbiased estimate of \mathbf{v}/R , since $\mathbb{E}[S_R(\mathbf{v})] = \mathbf{v}/R$.
347

348 We can now introduce our majority vote signSGD with momentum updates. First, we use the mo-
349 mentum gradient estimator at each node j as follows:

$$350 \quad 351 \quad \mathbf{v}_t^j = (1 - \beta) \mathbf{v}_{t-1}^j + \beta \nabla f_j(\mathbf{x}_t; \xi_t^j), \quad (9)$$

352 where β is the momentum parameter. Next, by communicating the gradient estimators with the
353 unbiased sign operation $S_G(\cdot)$, we update the decision variable as follows:

$$355 \quad 356 \quad 357 \quad \mathbf{x}_{t+1} = \mathbf{x}_t - \eta \operatorname{Sign} \left(\frac{1}{n} \sum_{j=1}^n S_G(\mathbf{v}_t^j) \right). \quad (10)$$

358 After applying $S_G(\cdot)$, the output is a sign vector, which can be efficiently transmitted between nodes.
359 The complete algorithm is described in Algorithm 2 (v1), called Majority Vote SignSGD with Mo-
360 mentum (MVSM). For $t = 1$, we initialize $\mathbf{v}_1^j = \nabla f_j(\mathbf{x}_1; \xi_1^j)$. MVSM-v1 is identical to MV-
361 sto-signSGD-SIM (with $\alpha = 0$) from Sun et al. (2023). However, our analysis yields stronger
362 convergence guarantees as stated below.

364 **Theorem 3** Under Assumptions 1, 6, 7 and 8, by setting that $\beta = \frac{1}{2}$ and $\eta = \mathcal{O} \left(\frac{1}{T^{1/2} d^{1/2}} \right)$, our
365 MVSM (v1) method ensures the following convergence:

$$367 \quad 368 \quad \mathbb{E} [\|\nabla f(\mathbf{x}_\tau)\|_1] \leq \mathcal{O} \left(\frac{d^{1/2}}{T^{1/2}} + \frac{d}{n^{1/2}} \right).$$

370 **Remark:** Our rate is superior to the previous result of $\mathcal{O} \left(\frac{d}{T^{1/4}} + \frac{d}{n^{1/2}} \right)$, indicating our significant
371 improvement over prior work (Sun et al., 2023) in both d and T dependencies.

372 By adjusting the learning rate, we can also obtain the following convergence guarantee.

374 **Theorem 4** Under Assumptions 1, 6, 7 and 8, by setting $\beta = \frac{1}{2}$ and $\eta = \mathcal{O}(n^{-1/2})$, our MVSM (v1)
375 method ensures:

$$377 \quad \mathbb{E} [\|\nabla f(\mathbf{x}_\tau)\|_1] \leq \mathcal{O} \left(\frac{n^{1/2}}{T} + \frac{d}{n^{1/2}} \right).$$

378 **Algorithm 2** Majority vote signSGD with momentum (MVSM)

```

379 1: Input: iteration number  $T$ , initial point  $\mathbf{x}_1$ 
380 2: for time step  $t = 1$  to  $T$  do
381 3:   On node  $j \in \{1, 2, \dots, n\}$ :
382 4:     Compute  $\mathbf{v}_t^j = (1 - \beta)\mathbf{v}_{t-1}^j + \beta \nabla f_j(\mathbf{x}_t; \xi_t^j)$ 
383 5:     Send  $S_G(\mathbf{v}_t^j)$  to the parameter server
384 6:   On parameter server:
385 7:     (v1) Send  $\mathbf{v}_t = \text{sign}\left(\frac{1}{n} \sum_{j=1}^n S_G(\mathbf{v}_t^j)\right)$  to all nodes
386 8:     (v2) Send  $\mathbf{v}_t = S_1\left(\frac{1}{n} \sum_{j=1}^n S_G(\mathbf{v}_t^j)\right)$  to all nodes
387 9:   On node  $j \in \{1, 2, \dots, n\}$ :
388 10:    Update the decision variable  $\mathbf{x}_{t+1} = \mathbf{x}_t - \eta \mathbf{v}_t$ 
389 11: end for
390 12: Select  $\tau$  uniformly at random from  $\{1, \dots, T\}$ 
391 13: Return  $\mathbf{x}_\tau$ 
392
393
394
```

395 **Remark:** This rate improves Theorem 3 when $T \geq \frac{n}{d}$, which is easily satisfied when d is large.

396 **Source of Theoretical Improvement:** The improvement for Algorithm 2 (v1) lies in deriving a
397 tighter error bound for the gradient estimator, i.e., $\epsilon_t = \left\| \nabla f(\mathbf{x}_t) - \frac{1}{n} \sum_{j=1}^n \mathbf{v}_t^j \right\|_2^2$. By carefully
398 analyzing the aggregated estimator $\frac{1}{n} \sum_{j=1}^n \mathbf{v}_t^j$, we obtain the recurrence: $\epsilon_{t+1} = (1 - \beta)\epsilon_t +$
399 $\frac{\sigma^2 \beta^2}{n} + \frac{2L^2 \eta^2 d}{\beta}$, which allows fast decay of ϵ_t with appropriate choices of β and η .

400 Although the above theorems achieve better convergence rates than previous methods, they do not
401 converge to zero as T increases. To address this issue, we replace the sign operation in the server with
402 the unbiased sign operation $S_1(\cdot)$ as defined in equation (8) with $R = 1$. The revised formulation
403 for the update is:

$$404 \mathbf{v}_t = S_1\left(\frac{1}{n} \sum_{j=1}^n S_G(\mathbf{v}_t^j)\right). \quad (11)$$

405 The corresponding algorithm is presented in Algorithm 2 (v2), with the only modification in Step 8.
406 We now present the convergence guarantee for this modified approach.

407 **Theorem 5** *Under Assumptions 1, 6, 7 and 8, by setting that $\eta = \mathcal{O}\left(\min\left\{\frac{1}{T^{1/2}d^{1/2}}, \frac{1}{T^{3/5}d^{1/5}}\right\}\right)$ and $\beta = \mathcal{O}\left(\eta^{2/3}d^{1/3}\right)$, the MVSM (v2) method ensures the following convergence:*

$$408 \mathbb{E} [\|\nabla f(\mathbf{x}_\tau)\|_2] \leq \mathcal{O}\left(\max\left\{\frac{d^{1/4}}{T^{1/4}}, \frac{d^{1/10}}{T^{1/5}}\right\}\right).$$

410 **Remark:** This convergence rate approaches zero as $T \rightarrow \infty$, and significantly improves upon the
411 previous result of $\mathcal{O}\left(\frac{d^{3/8}}{T^{1/8}}\right)$ (Jin et al., 2021), in terms of both T and d .

412 **Source of Theoretical Improvement:** The improved rate stems from the unbiased estimation of
413 the full gradient, allowing us to use $\mathbb{E} \left[S_1\left(\frac{1}{n} \sum_{j=1}^n S_G(\mathbf{v}_t^j)\right) \right] = \frac{1}{nG} \sum_{j=1}^n \mathbf{v}_t^j$ in the analysis. In
414 contrast, prior works (Jin et al., 2021; Sun et al., 2023) use biased sign operators on the server, which
415 leads to looser bounds and higher complexities.

416 **5 EXPERIMENTS**

417 In this section, we evaluate the performance of our methods through numerical experiments. We
418 first assess the Signum algorithm on the image classification task in a centralized setting, and then
419 test the proposed MVSM method in the distributed learning environment. Finally, we experiment on
420 the fine-tuning task for large language models. All experiments are conducted on NVIDIA GeForce

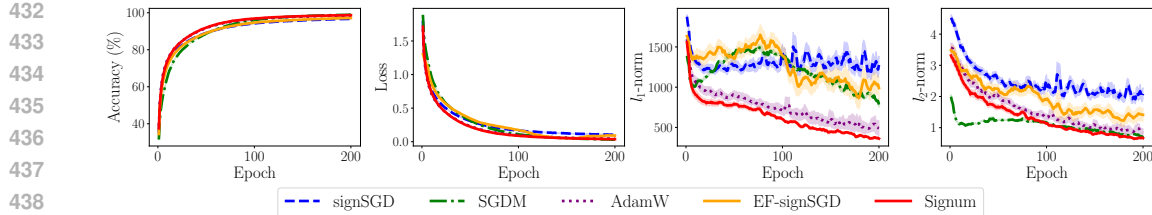


Figure 1: Results for CIFAR-10 dataset in the centralized environment.

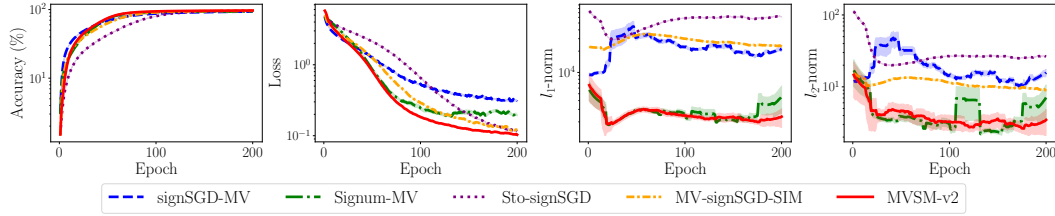


Figure 2: Results for CIFAR-100 dataset in the distributed environment.

RTX 3090 GPUs, and results are averaged over 10 runs, with shaded regions representing the standard deviation.

5.1 IMAGE CLASSIFICATION IN THE CENTRALIZED ENVIRONMENT

We validate the effectiveness of sign-based methods on the image classification task. Specifically, we train a ResNet-18 model (He et al., 2016) on the CIFAR-10 dataset (Krizhevsky, 2009) and compare our method against signSGD (Bernstein et al., 2018), SGDM (Sutskever et al., 2013), AdamW (Kingma & Ba, 2015; Loshchilov & Hutter, 2019), and signSGD with error feedback (i.e., EF-signSGD) (Karimireddy et al., 2019). For SGDM and AdamW, we use the official PyTorch implementations (Paszke et al., 2019). For each optimizer method, hyperparameters are determined through grid search. Specifically, the momentum parameter β is selected from the set $\{0.9, 0.5, 0.1, 0.01\}$, and the learning rate η is chosen from the set $\{0.5, 0.25, 0.1, 0.05, 0.025, 0.01\} \times 10^{-2}$.

Figure 1 reports the training loss, accuracy, and the l_1 - and l_2 -norms of the gradients. In terms of loss and accuracy, the Signum method converges fastest even among the algorithms that update with full gradient information. Additionally, the Signum method results in the most rapid reduction of both l_1 and l_2 gradient norms. These findings are consistent with our theoretical results, further highlighting the effectiveness of momentum-based sign methods in accelerating convergence and improving optimization efficiency.

5.2 IMAGE CLASSIFICATION IN THE DISTRIBUTED ENVIRONMENT

Next, we evaluate our method in the distributed setting. We train a ResNet-50 model (He et al., 2016) on the CIFAR-100 dataset (Krizhevsky, 2009) across 8 nodes. We compare our newly proposed MVSM-v2 method against signSGD (with Majority Vote) (Bernstein et al., 2018), Signum (with Majority Vote) (Bernstein et al., 2019), Sto-signSGD (Jin et al., 2021), and MV-signSGD-SIM (Sun et al., 2023). Also note that the MV-signSGD algorithm is identical to our MVSM-v1 method. The hyperparameters are searched in the same way as in Section 5.1.

Figure 2 presents the training loss, accuracy, and the l_1 - and l_2 -norms of the gradients. Our MVSM-v2 algorithm achieves the lowest loss and highest accuracy, while also exhibiting sparser gradients compared to other methods. In contrast, sign-based optimizers that do not incorporate momentum updates—specifically, signSGD-MV and Sto-signSGD—exhibit poor performance and produce significantly larger gradients. These results further underscore the advantage of integrating momentum into sign-based optimization methods.

486
487
488 Table 4: Training losses of finetuning GPT-2 and Qwen3 on the Alpaca dataset.
489
490
491

Method	SGDM	signSGD	EF-signSGD	AdamW	Signum
GPT-2	2.509±.005	2.236±.004	2.267±.003	2.183±.001	2.176±.002
Qwen3	1.677±.006	1.610±.003	1.609±.005	1.592±.002	1.592±.001

492
493
494 5.3 INSTRUCTION FOLLOWING FINE-TUNING FOR LARGE LANGUAGE MODELS
495

496 Finally, we conduct experiments on fine-tuning
497 LLMs to evaluate the high-dimensional and practical
498 usage of sign-based optimizers. Specifically,
499 we compare signSGD, SGDM, AdamW, and EF-
500 signSGD with our Signum method on the GPT-
501 2 (Radford et al., 2019) and Qwen3-0.6B (Yang
502 et al., 2025) models. These optimization algo-
503 rithms are evaluated on the Alpaca dataset (Taori
504 et al., 2023), which consists of 52000 instruction-
505 following question-answer pairs. Throughout the
506 experiments, we follow a similar setup as Liu
507 et al. (2025c) and set the hyperparameters listed
508 in Table 3. All other settings remain at their
509 `transformers==4.52.4` defaults. To cut memory usage and speed up training, we leverage the
510 LMFlow toolbox (Diao et al., 2024). For the remaining hyperparameters, we either adopt the values
511 from the original paper or perform a grid search. For AdamW, we keep $\beta_1 = 0.9$, $\beta_2 = 0.95$, the de
512 facto standard for training LLMs such as LLaMA (Touvron et al., 2023) and AMD-Llama-135M,
513 whose model size closely matches ours. For every other optimizer that maintains a momentum state,
514 we search $\beta_1 \in \{0.99, 0.95, 0.9, 0.75, 0.5, 0\}$ (represents $1 - \beta$ in Algorithm 1). All methods explore
515 learning rates in $\{1, 5\} \times \{1e1, 1e0, 1e-1, 1e-2, 1e-3, 1e-4, 1e-5, 1e-6\}$.

516 The experimental results are listed in Table 4, which shows that our method yields lower training loss
517 compared to other baselines. We notice that Signum has a similar performance to AdamW, which
518 is consistent with the empirical observations by Kunstner et al. (2023); Chen et al. (2023). These
519 findings highlight the practical effect of sign-based methods for training complex, high-dimensional
520 models. The optimal hyperparameters for each algorithm can be found in Appendix E.1. We also
521 conduct hyperparameter sensitivity analysis in Appendix E.2, and empirical validation of Assump-
522 tion 8 in Appendix E.3.

523 6 CONCLUSION

524 In this paper, we demonstrate that signSGD with momentum update can achieve a convergence
525 rate of $\mathcal{O}(T^{-1/4})$ without requiring large batch sizes or assuming unimodal symmetric noise.
526 When analyzed under the l_2 -smoothness assumption, our method achieves a convergence rate of
527 $\mathcal{O}(d^{1/2}T^{-1/4})$, which improves upon the previous rate of $\mathcal{O}(dT^{-1/4})$. In distributed settings, we
528 establish convergence rates of $\mathcal{O}\left(\frac{d^{1/2}}{T^{1/2}} + \frac{d}{n^{1/2}}\right)$ and $\mathcal{O}\left(\max\left\{\frac{d^{1/4}}{T^{1/4}}, \frac{d^{1/10}}{T^{1/5}}\right\}\right)$, which significantly
529 outperform prior results of $\mathcal{O}\left(\frac{d}{T^{1/4}} + \frac{d}{n^{1/2}}\right)$ and $\mathcal{O}\left(\frac{d^{3/8}}{T^{1/8}}\right)$. Finally, numerical experiments in dif-
530 ferent learning environments also validate the effectiveness of the proposed method.

531
532
533
534
535
536
537
538
539 Table 3: Hyperparameter configurations.

Hyperparameter	Value
weight decay	0.1
batch size	256
max sequence length	512
gradient accumulation steps	1
epochs	1.0
learning rate schedule	cosine decay

540 REPRODUCIBILITY STATEMENT
541

542 We provide clear explanations of all assumptions and include complete proofs of our theoretical
543 claims in the appendix. For the experimental results, we specify the dataset, baseline methods, and
544 hyperparameter choices.

545
546 THE USE OF LLMs
547

548 We used large language models (LLMs) solely for minor language polishing of the manuscript. The
549 LLMs did not contribute to research ideation, algorithm design, theoretical analysis, or experimental
550 work. Their role was strictly limited to assisting with improving readability and grammar.

551
552 REFERENCES

553 Yossi Arjevani, Yair Carmon, John C. Duchi, Dylan J. Foster, Nathan Srebro, and Blake E. Wood-
554 worth. Lower bounds for non-convex stochastic optimization. *Mathematical Programming*, 199
555 (1-2):165–214, 2023.

556 Jeremy Bernstein, Yu-Xiang Wang, Kamyar Azizzadenesheli, and Animashree Anandkumar.
557 signSGD: Compressed optimisation for non-convex problems. In *Proceedings of the 35th In-
558 ternational Conference on Machine Learning*, pp. 560–569, 2018.

559 Jeremy Bernstein, Jiawei Zhao, Kamyar Azizzadenesheli, and Anima Anandkumar. signSGD with
560 majority vote is communication efficient and fault tolerant. In *International Conference on Learn-
561 ing Representations*, 2019.

562 Xiangning Chen, Chen Liang, Da Huang, Esteban Real, Kaiyuan Wang, Hieu Pham, Xuanyi Dong,
563 Thang Luong, Cho-Jui Hsieh, Yifeng Lu, and Quoc V Le. Symbolic discovery of optimization
564 algorithms. In *Advances in Neural Information Processing Systems 36*, pp. 49205–49233, 2023.

565 Shizhe Diao, Rui Pan, Hanze Dong, KaShun Shum, Jipeng Zhang, Wei Xiong, and Tong Zhang.
566 Lmflow: An extensible toolkit for finetuning and inference of large foundation models. In *Pro-
567 ceedings of the 2024 Conference of the North American Chapter of the Association for Com-
568 putational Linguistics: Human Language Technologies (Volume 3: System Demonstrations)*, pp.
569 116–127, 2024. URL <https://github.com/OptimalScale/LMFlow>.

570 Yiming Dong, Huan Li, and Zhouchen Lin. Convergence rate analysis of lion. *ArXiv e-prints*,
571 arXiv:2411.07724, 2024.

572 John Duchi, Elad Hazan, and Yoram Singer. Adaptive subgradient methods for online learning and
573 stochastic optimization. *Journal of Machine Learning Research*, 12(61):2121–2159, 2011.

574 Cong Fang, Chris Junchi Li, Zhouchen Lin, and Tong Zhang. SPIDER: Near-optimal non-convex
575 optimization via stochastic path-integrated differential estimator. In *Advances in Neural Infor-
576 mation Processing Systems 31*, pp. 689–699, 2018.

577 Saeed Ghadimi and Guanghui Lan. Stochastic first- and zeroth-order methods for nonconvex
578 stochastic programming. *SIAM Journal on Optimization*, 23(4):2341–2368, 2013.

579 Kaiming He, Xiangyu Zhang, Shaoqing Ren, and Jian Sun. Deep residual learning for image recog-
580 nition. In *Proceedings of the IEEE/CVF Conference on Computer Vision and Pattern Recognition*,
581 pp. 770–778, 2016.

582 Ruichen Jiang, Devyani Maladkar, and Aryan Mokhtari. Provable complexity improvement of ada-
583 grad over sgd: Upper and lower bounds in stochastic non-convex optimization. In *Proceedings of
584 Thirty Eighth Conference on Learning Theory*, volume 291, pp. 3124–3158, 2025.

585 Wei Jiang, Sifan Yang, Wenhao Yang, and Lijun Zhang. Efficient sign-based optimization: Acceler-
586 ating convergence via variance reduction. In *Advances in Neural Information Processing Systems*
587 37, pp. 33891–33932, 2024.

588 Richeng Jin, Yufan Huang, Xiaofan He, Huaiyu Dai, and Tianfu Wu. Stochastic-Sign SGD for
589 federated learning with theoretical guarantees. *ArXiv e-prints*, arXiv:2002.10940, 2021.

594 Sai Praneeth Karimireddy, Quentin Rebjock, Sebastian Stich, and Martin Jaggi. Error feedback
 595 fixes SignSGD and other gradient compression schemes. In *Proceedings of the 36th International*
 596 *Conference on Machine Learning*, pp. 3252–3261, 2019.

597 Diederik P. Kingma and Jimmy Lei Ba. Adam: A method for stochastic optimization. In *International*
 598 *Conference on Learning Representations*, 2015.

600 Atli Kosson, Bettina Messmer, and Martin Jaggi. Rotational equilibrium: How weight decay bal-
 601 ances learning across neural networks. In *Proceedings of the 41st International Conference on*
 602 *Machine Learning*, pp. 25333–25369, 2024.

603 Alex Krizhevsky. Learning multiple layers of features from tiny images. *Masters Thesis, Department*
 604 *of Computer Science, University of Toronto*, 2009.

605 Frederik Kunstner, Jacques Chen, Jonathan Wilder Lavington, and Mark Schmidt. Noise is not the
 606 main factor behind the gap between sgd and adam on transformers, but sign descent might be. In
 607 *International Conference on Learning Representations*, 2023.

609 Jingyuan Liu, Jianlin Su, Xingcheng Yao, Zhejun Jiang, Guokun Lai, Yulun Du, Yidao Qin,
 610 Weixin Xu, Enzhe Lu, Junjie Yan, et al. Muon is scalable for llm training. *arXiv preprint*
 611 *arXiv:2502.16982*, 2025a.

612 Sijia Liu, Pin-Yu Chen, Xiangyi Chen, and Mingyi Hong. signSGD via zeroth-order oracle. In
 613 *International Conference on Learning Representations*, 2019.

615 Yifeng Liu, Angela Yuan, and Quanquan Gu. Mars-m: When variance reduction meets matrices.
 616 *arXiv preprint arXiv:2510.21800*, 2025b.

617 Yuxing Liu, Rui Pan, and Tong Zhang. Adagrad under anisotropic smoothness. In *International*
 618 *Conference on Learning Representations*, 2025c.

620 Ilya Loshchilov and Frank Hutter. SGDR: Stochastic gradient descent with warm restarts. In *Inter-*
 621 *national Conference on Learning Representations*, 2017.

622 Ilya Loshchilov and Frank Hutter. Decoupled weight decay regularization. In *International Confer-*
 623 *ence on Learning Representations*, 2019.

625 Adam Paszke, Sam Gross, Francisco Massa, Adam Lerer, James Bradbury, Gregory Chanan, Trevor
 626 Killeen, Zeming Lin, Natalia Gimelshein, Luca Antiga, Alban Desmaison, Andreas Kopf, Edward
 627 Yang, Zachary DeVito, Martin Raison, Alykhan Tejani, Sasank Chilamkurthy, Benoit Steiner,
 628 Lu Fang, Junjie Bai, and Soumith Chintala. Pytorch: An imperative style, high-performance deep
 629 learning library. In *Advances in Neural Information Processing Systems 32*, 2019.

630 Alec Radford, Jeffrey Wu, Rewon Child, David Luan, Dario Amodei, Ilya Sutskever, et al. Language
 631 models are unsupervised multitask learners. *OpenAI blog*, 1(8):9, 2019.

632 Mher Safaryan and Peter Richtarik. Stochastic sign descent methods: New algorithms and better
 633 theory. In *Proceedings of the 38th International Conference on Machine Learning*, pp. 9224–
 634 9234, 2021.

636 Tao Sun, Qingsong Wang, Dongsheng Li, and Bao Wang. Momentum ensures convergence of
 637 SIGNSGD under weaker assumptions. In *Proceedings of the 40th International Conference on*
 638 *Machine Learning*, pp. 33077–33099, 2023.

639 Ilya Sutskever, James Martens, George Dahl, and Geoffrey Hinton. On the importance of initial-
 640 ization and momentum in deep learning. In *Proceedings of the 30th International Conference on*
 641 *Machine Learning*, pp. 1139–1147, 2013.

642 Zhiwei Tang, Yanmeng Wang, and Tsung-Hui Chang. z-signfedavg: A unified stochastic sign-
 643 based compression for federated learning. *Proceedings of the AAAI Conference on Artificial*
 644 *Intelligence*, 38(14):15301–15309, 2024.

646 Rohan Taori, Ishaan Gulrajani, Tianyi Zhang, Yann Dubois, Xuechen Li, Carlos Guestrin, Percy
 647 Liang, and Tatsunori B Hashimoto. Stanford alpaca: An instruction-following llama model, 2023.
 URL https://github.com/tatsu-lab/stanford_alpaca.

648 Hugo Touvron, Thibaut Lavril, Gautier Izacard, Xavier Martinet, Marie-Anne Lachaux, Timothée
649 Lacroix, Baptiste Rozière, Naman Goyal, Eric Hambro, Faisal Azhar, et al. Llama: Open and
650 efficient foundation language models. *arXiv preprint arXiv:2302.13971*, 2023.

651
652 Zhe Wang, Kaiyi Ji, Yi Zhou, Yingbin Liang, and Vahid Tarokh. SpiderBoost and momentum:
653 Faster variance reduction algorithms. In *Advances in Neural Information Processing Systems 32*,
654 pp. 2406–2416, 2019.

655 An Yang, Anfeng Li, Baosong Yang, Beichen Zhang, Binyuan Hui, Bo Zheng, Bowen Yu,
656 Chang Gao, Chengan Huang, Chenxu Lv, et al. Qwen3 technical report. *arXiv preprint*
657 *arXiv:2505.09388*, 2025.

658

659

660

661

662

663

664

665

666

667

668

669

670

671

672

673

674

675

676

677

678

679

680

681

682

683

684

685

686

687

688

689

690

691

692

693

694

695

696

697

698

699

700

701

APPENDIX

A PROOF OF THEOREM 1

According to Assumption 2 and considering the update $\mathbf{x}_{t+1} - \mathbf{x}_t = -\eta \text{Sign}(\mathbf{v}_t)$, we know that

$$\begin{aligned}
 f(\mathbf{x}_{t+1}) - f(\mathbf{x}_t) &\leq \langle \nabla f(\mathbf{x}_t), \mathbf{x}_{t+1} - \mathbf{x}_t \rangle + \frac{1}{2} \sum_{i=1}^d L_i ([\mathbf{x}_{t+1}]_i - [\mathbf{x}_t]_i)^2 \\
 &\leq -\langle \nabla f(\mathbf{x}_t), \eta \text{Sign}(\mathbf{v}_t) \rangle + \frac{\eta^2}{2} \sum_{i=1}^d L_i (\text{Sign}(\mathbf{v}_t)_i)^2 \\
 &\leq -\langle \nabla f(\mathbf{x}_t), \eta \text{Sign}(\nabla f(\mathbf{x}_t)) \rangle \\
 &\quad + \eta \langle \nabla f(\mathbf{x}_t), \text{Sign}(\nabla f(\mathbf{x}_t)) - \text{Sign}(\mathbf{v}_t) \rangle + \frac{\eta^2}{2} \sum_{i=1}^d L_i \\
 &\leq -\eta \|\nabla f(\mathbf{x}_t)\|_1 + 2\eta \|\nabla f(\mathbf{x}_t) - \mathbf{v}_t\|_1 + \frac{\eta^2}{2} \sum_{i=1}^d L_i,
 \end{aligned}$$

where the last inequality is due to

$$\begin{aligned}
 &\langle \nabla f(\mathbf{x}_t), \text{Sign}(\nabla f(\mathbf{x}_t)) - \text{Sign}(\mathbf{v}_t) \rangle \\
 &= \sum_{i=1}^d [\nabla f(\mathbf{x}_t)]_i \cdot (\text{Sign}[\nabla f(\mathbf{x}_t)]_i - \text{Sign}[\mathbf{v}_t]_i) \\
 &\leq \sum_{i=1}^d 2 [\nabla f(\mathbf{x}_t)]_i \cdot \mathbb{I}(\text{Sign}([\nabla f(\mathbf{x}_t)]_i) \neq \text{Sign}[\mathbf{v}_t]_i) \\
 &\leq \sum_{i=1}^d 2 |[\nabla f(\mathbf{x}_t)]_i - [\mathbf{v}_t]_i| \cdot \mathbb{I}(\text{Sign}[\nabla f(\mathbf{x}_t)]_i \neq \text{Sign}[\mathbf{v}_t]_i) \\
 &\leq \sum_{i=1}^d 2 |[\nabla f(\mathbf{x}_t)]_i - [\mathbf{v}_t]_i| = 2 \|\nabla f(\mathbf{x}_t) - \mathbf{v}_t\|_1.
 \end{aligned}$$

Rearranging the obtained relation and summing up yields

$$\mathbb{E} \left[\frac{1}{T} \sum_{t=1}^T \|\nabla f(\mathbf{x}_t)\|_1 \right] \leq \frac{\Delta_f}{\eta T} + 2\mathbb{E} \left[\frac{1}{T} \sum_{t=1}^T \|\nabla f(\mathbf{x}_t) - \mathbf{v}_t\|_1 \right] + \frac{\eta}{2} \sum_{i=1}^d L_i, \quad (12)$$

where we define $\Delta_f = f(\mathbf{x}_1) - f_*$.

Next, we proceed to bound the error term $\mathbb{E} \left[\frac{1}{T} \sum_{t=1}^T \|\nabla f(\mathbf{x}_t) - \mathbf{v}_t\|_1 \right]$. For convenience, we define the following notations:

$$\boldsymbol{\epsilon}_t := \mathbf{v}_t - \nabla f(\mathbf{x}_t), \quad \mathbf{n}_t := \nabla f(\mathbf{x}_t; \xi_t) - \nabla f(\mathbf{x}_t), \quad \mathbf{s}_t := \nabla f(\mathbf{x}_{t-1}) - \nabla f(\mathbf{x}_t).$$

By definition, we have

$$\begin{aligned}
 \boldsymbol{\epsilon}_t &= \mathbf{v}_t - \nabla f(\mathbf{x}_t) = (1 - \beta) \mathbf{v}_{t-1} + \beta \nabla f(\mathbf{x}_t; \xi_t) - \nabla f(\mathbf{x}_t) \\
 &= (1 - \beta) (\mathbf{v}_{t-1} - \nabla f(\mathbf{x}_{t-1})) + (1 - \beta) (\nabla f(\mathbf{x}_{t-1}) - \nabla f(\mathbf{x}_t)) + \beta (\nabla f(\mathbf{x}_t; \xi_t) - \nabla f(\mathbf{x}_t)) \\
 &= (1 - \beta) \boldsymbol{\epsilon}_{t-1} + (1 - \beta) \mathbf{s}_t + \beta \mathbf{n}_t.
 \end{aligned}$$

Performing this recursively yields

$$\boldsymbol{\epsilon}_t = (1 - \beta)^{t-1} \mathbf{n}_1 + \beta \sum_{k=2}^t (1 - \beta)^{t-k} \mathbf{n}_k + \sum_{k=2}^t (1 - \beta)^{t-k+1} \mathbf{s}_k,$$

756 where we use the fact that $\epsilon_1 = \mathbf{v}_1 - \nabla f(\mathbf{x}_1) = \nabla f(\mathbf{x}_1; \xi_1) - \nabla f(\mathbf{x}_1) = \mathbf{n}_1$. We bound ϵ_t via two
757 terms A_t and B_t as follows:

$$759 \mathbb{E} [\|\epsilon_t\|_1] \leq \underbrace{\mathbb{E} \left[\left\| (1 - \beta)^{t-1} \mathbf{n}_1 + \beta \sum_{k=2}^t (1 - \beta)^{t-k} \mathbf{n}_k \right\|_1 \right]}_{A_t} + \underbrace{\mathbb{E} \left[\left\| \sum_{k=2}^t (1 - \beta)^{t-k+1} \mathbf{s}_k \right\|_1 \right]}_{B_t}$$

763 Firstly, we cope with A_t following the similar procedure as in Liu et al. (2025c, Lemma E.2).
764 We denote the i -th element of the vector \mathbf{n}_t by $\mathbf{n}_{t,i}$. By the Cauchy–Schwarz inequality, for any
765 $\lambda_1, \dots, \lambda_d > 0$, it holds that

$$\begin{aligned} 767 & \mathbb{E} \left[\left\| (1 - \beta)^{t-1} \mathbf{n}_1 + \beta \sum_{k=2}^t (1 - \beta)^{t-k} \mathbf{n}_k \right\|_1^2 \right] \\ 768 & \leq \left(\sum_{i=1}^d \lambda_i \right) \sum_{i=1}^d \frac{1}{\lambda_i} \mathbb{E} \left[(1 - \beta)^{t-1} \mathbf{n}_{1,i} + \beta \sum_{k=2}^t (1 - \beta)^{t-k} \mathbf{n}_{k,i} \right]^2 \\ 769 & = \left(\sum_{i=1}^d \lambda_i \right) \sum_{i=1}^d \frac{1}{\lambda_i} \left((1 - \beta)^{2t-2} \mathbb{E} [\mathbf{n}_{1,i}^2] + \beta^2 \sum_{k=2}^t (1 - \beta)^{2(t-k)} \mathbb{E} [\mathbf{n}_{k,i}^2] \right) \\ 770 & \leq \left(\sum_{i=1}^d \lambda_i \right) \sum_{i=1}^d \frac{1}{\lambda_i} \left((1 - \beta)^{2t-2} \sigma_i^2 + \beta^2 \sum_{k=2}^t (1 - \beta)^{2(t-k)} \sigma_i^2 \right) \\ 771 & \leq \left(\sum_{i=1}^d \lambda_i \right) \sum_{i=1}^d \frac{\sigma_i^2}{\lambda_i} \left((1 - \beta)^{2t-2} + \frac{\beta}{2 - \beta} \right), \end{aligned}$$

782 where the equality is due to $\mathbb{E} [\mathbf{n}_{s,i} \cdot \mathbf{n}_{t,i}] = 0, \forall s < t \in [T], \forall i \in [d]$; the second inequality is due
783 to Assumption 3. Denoting by $\sigma = [\sigma_1, \dots, \sigma_d]^\top$ and setting $\lambda_i = \sigma_i$, we obtain

$$\begin{aligned} 784 A_t & \leq \sqrt{\mathbb{E} \left[\left\| (1 - \beta)^{t-1} \mathbf{n}_1 + \beta \sum_{k=2}^t (1 - \beta)^{t-k} \mathbf{n}_k \right\|_1^2 \right]} \\ 785 & \leq \sqrt{\left((1 - \beta)^{2t-2} + \frac{\beta}{2 - \beta} \right) \|\sigma\|_1^2} \leq \left((1 - \beta)^{t-1} + \sqrt{\frac{\beta}{2 - \beta}} \right) \|\sigma\|_1, \end{aligned}$$

791 where we make use of $\mathbb{E}^2[X] \leq \mathbb{E}[X^2]$ and $\sqrt{a + b} \leq \sqrt{a} + \sqrt{b}, \forall a, b \geq 0$.

793 Secondly, we cope with B_t as the following:

$$794 B_t \leq \sum_{k=2}^t (1 - \beta)^{t-k+1} \mathbb{E} [\|\mathbf{s}_k\|_1] \leq 2\eta \|\vec{L}\|_1 \sum_{k=2}^t (1 - \beta)^{t-k+1} \leq \frac{2(1 - \beta)\eta \|\vec{L}\|_1}{\beta},$$

797 where the second inequality uses

$$799 \mathbb{E} [\|\mathbf{s}_k\|_1] = \|\nabla f(\mathbf{x}_{t-1}) - \nabla f(\mathbf{x}_t)\|_1 = \|\nabla f(\mathbf{x}_t + \eta \text{Sign}(\mathbf{v}_{t-1})) - \nabla f(\mathbf{x}_t)\|_1 \leq 2\eta \|\vec{L}\|_1,$$

800 which is due to the following lemma.

801 **Lemma 1** (Lemma F.3. in Bernstein et al. (2018)) *Under Assumption 2, for any sign vector $\mathbf{s} \in \{-1, 1\}^d$, any $\mathbf{x} \in \mathbb{R}^d$ and any η*

$$804 \|\nabla f(\mathbf{x} + \eta \mathbf{s}) - \nabla f(\mathbf{x})\|_1 \leq 2\eta \|\vec{L}\|_1.$$

806 Now it suffices to combine the bounds for A_t, B_t :

$$808 \frac{1}{T} \sum_{t=1}^T \mathbb{E} [\|\epsilon_t\|_1] \leq \frac{1}{T} \sum_{t=1}^T (A_t + B_t) \leq \left(\frac{1}{T\beta} + \sqrt{\frac{\beta}{2 - \beta}} \right) \|\sigma\|_1 + \frac{2(1 - \beta)\eta \|\vec{L}\|_1}{\beta},$$

810 where we make use of $\sum_{t=1}^T (1 - \beta)^{t-1} \leq 1/\beta$. Plugging this relation into equation 12 yields
 811

$$812 \mathbb{E} \left[\frac{1}{T} \sum_{t=1}^T \|\nabla f(\mathbf{x}_t)\|_1 \right] \leq \frac{\Delta_f}{\eta T} + \frac{\eta \|\vec{L}\|_1}{2} + 2 \|\boldsymbol{\sigma}\|_1 \left(\frac{1}{T\beta} + \sqrt{\frac{\beta}{2-\beta}} \right) + \frac{4(1-\beta)\eta \|\vec{L}\|_1}{\beta}$$

815 Setting $\eta = \sqrt{\frac{\Delta_f}{\|\vec{L}\|_1}} \cdot T^{-3/4}$, $\beta = \frac{1}{\sqrt{T}}$, we obtain
 816

$$817 \mathbb{E} [\|\nabla f(\mathbf{x}_\tau)\|_1] \leq \sqrt{\|\vec{L}\|_1 \Delta_f} \left(\frac{5}{T^{1/4}} + \frac{1}{2T^{3/4}} \right) + 2 \|\boldsymbol{\sigma}\|_1 \left(\frac{1}{T^{1/4}} + \frac{1}{\sqrt{T}} \right) = \mathcal{O} \left(\frac{1}{T^{1/4}} \right).$$

820 B PROOF OF THEOREM 2

822 Firstly, due to the l_2 -smoothness assumption (Assumption 4), we have that
 823

$$\begin{aligned} 824 \quad & f(\mathbf{x}_{t+1}) \\ 825 \quad & \leq f(\mathbf{x}_t) + \langle \nabla f(\mathbf{x}_t), \mathbf{x}_{t+1} - \mathbf{x}_t \rangle + \frac{L}{2} \|\mathbf{x}_{t+1} - \mathbf{x}_t\|^2 \\ 826 \quad & = f(\mathbf{x}_t) - \eta \langle \nabla f(\mathbf{x}_t), \text{Sign}(\mathbf{v}_t) \rangle + \frac{\eta^2 L}{2} \|\text{Sign}(\mathbf{v}_t)\|^2 \\ 827 \quad & \leq f(\mathbf{x}_t) + \eta \langle \nabla f(\mathbf{x}_t), \text{Sign}(\nabla f(\mathbf{x}_t)) - \text{Sign}(\mathbf{v}_t) \rangle - \eta \langle \nabla f(\mathbf{x}_t), \text{Sign}(\nabla f(\mathbf{x}_t)) \rangle + \frac{\eta^2 L d}{2} \\ 828 \quad & = f(\mathbf{x}_t) + \eta \langle \nabla f(\mathbf{x}_t), \text{Sign}(\nabla f(\mathbf{x}_t)) - \text{Sign}(\mathbf{v}_t) \rangle - \eta \|\nabla f(\mathbf{x}_t)\|_1 + \frac{\eta^2 L d}{2} \\ 829 \quad & = f(\mathbf{x}_t) + \eta \sum_{i=1}^d \langle [\nabla f(\mathbf{x}_t)]_i, \text{Sign}([\nabla f(\mathbf{x}_t)]_i) - \text{Sign}([\mathbf{v}_t]_i) \rangle - \eta \|\nabla f(\mathbf{x}_t)\|_1 + \frac{\eta^2 L d}{2} \\ 830 \quad & \leq f(\mathbf{x}_t) + \eta \sum_{i=1}^d 2 |[\nabla f(\mathbf{x}_t)]_i| \cdot \mathbb{I}(\text{Sign}([\nabla f(\mathbf{x}_t)]_i) \neq \text{Sign}([\mathbf{v}_t]_i)) - \eta \|\nabla f(\mathbf{x}_t)\|_1 \\ 831 \quad & \quad + \frac{\eta^2 L d}{2} \\ 832 \quad & \leq f(\mathbf{x}_t) + \eta \sum_{i=1}^d 2 |[\nabla f(\mathbf{x}_t)]_i - [\mathbf{v}_t]_i| \cdot \mathbb{I}(\text{Sign}([\nabla f(\mathbf{x}_t)]_i) \neq \text{Sign}([\mathbf{v}_t]_i)) - \eta \|\nabla f(\mathbf{x}_t)\|_1 \\ 833 \quad & \quad + \frac{\eta^2 L d}{2} \\ 834 \quad & \leq f(\mathbf{x}_t) + \eta \sum_{i=1}^d 2 |[\nabla f(\mathbf{x}_t)]_i - [\mathbf{v}_t]_i| - \eta \|\nabla f(\mathbf{x}_t)\|_1 + \frac{\eta^2 L d}{2} \\ 835 \quad & = f(\mathbf{x}_t) + 2\eta \|\nabla f(\mathbf{x}_t) - \mathbf{v}_t\|_1 - \eta \|\nabla f(\mathbf{x}_t)\|_1 + \frac{\eta^2 L d}{2} \\ 836 \quad & \leq f(\mathbf{x}_t) + 2\eta \sqrt{d} \|\nabla f(\mathbf{x}_t) - \mathbf{v}_t\| - \eta \|\nabla f(\mathbf{x}_t)\|_1 + \frac{\eta^2 L d}{2}. \end{aligned} \tag{13}$$

837 Summing up and rearranging the equation (13), we derive:
 838

$$\begin{aligned} 839 \quad & \mathbb{E} \left[\frac{1}{T} \sum_{t=1}^T \|\nabla f(\mathbf{x}_t)\|_1 \right] \\ 840 \quad & \leq \frac{f(\mathbf{x}_1) - f(\mathbf{x}_{T+1})}{\eta T} + 2\sqrt{d} \cdot \mathbb{E} \left[\frac{1}{T} \sum_{t=1}^T \|\nabla f(\mathbf{x}_t) - \mathbf{v}_t\| \right] + \frac{\eta L d}{2} \\ 841 \quad & \leq \frac{\Delta_f}{\eta T} + 2\sqrt{d} \cdot \sqrt{\mathbb{E} \left[\frac{1}{T} \sum_{t=1}^T \|\nabla f(\mathbf{x}_t) - \mathbf{v}_t\|^2 \right]} + \frac{\eta L d}{2}. \end{aligned} \tag{14}$$

864 where we define $\Delta_f = f(\mathbf{x}_1) - f_*$, and the second inequality is due to Jensen's Inequality.
 865

866 Next, we can bound the term $\mathbb{E} \left[\frac{1}{T} \sum_{t=1}^T \|\nabla f(\mathbf{x}_t) - \mathbf{v}_t\|^2 \right]$ as follows.
 867

$$\begin{aligned}
 870 \mathbb{E} \left[\|\nabla f(\mathbf{x}_{t+1}) - \mathbf{v}_{t+1}\|^2 \right] &= \mathbb{E} \left[\|(1-\beta)\mathbf{v}_t + \beta \nabla f(\mathbf{x}_{t+1}; \xi_{t+1}) - \nabla f(\mathbf{x}_{t+1})\|^2 \right] \\
 871 &= \mathbb{E} \left[\|(1-\beta)(\mathbf{v}_t - \nabla f(\mathbf{x}_t)) + \beta (\nabla f(\mathbf{x}_{t+1}; \xi_{t+1}) - \nabla f(\mathbf{x}_{t+1})) \right. \\
 872 &\quad \left. + (1-\beta)(\nabla f(\mathbf{x}_t) - \nabla f(\mathbf{x}_{t+1}))\|^2 \right] \\
 873 &= (1-\beta)^2 \mathbb{E} \left[\|\mathbf{v}_t - \nabla f(\mathbf{x}_t) + \nabla f(\mathbf{x}_t) - \nabla f(\mathbf{x}_{t+1})\|^2 \right] \\
 874 &\quad + \beta^2 \mathbb{E} \left[\|\nabla f(\mathbf{x}_{t+1}; \xi_{t+1}) - \nabla f(\mathbf{x}_{t+1})\|^2 \right] \\
 875 &\leq (1-\beta)^2 (1+\beta) \mathbb{E} \left[\|\mathbf{v}_t - \nabla f(\mathbf{x}_t)\|^2 \right] \\
 876 &\quad + (1-\beta)^2 (1 + \frac{1}{\beta}) \mathbb{E} \left[\|\nabla f(\mathbf{x}_t) - \nabla f(\mathbf{x}_{t+1})\|^2 \right] + \beta^2 \sigma^2 \\
 877 &\leq (1-\beta) \mathbb{E} \left[\|\mathbf{v}_t - \nabla f(\mathbf{x}_t)\|^2 \right] + \frac{2L^2}{\beta} \|\mathbf{x}_{t+1} - \mathbf{x}_t\|^2 + \beta^2 \sigma^2 \\
 878 &\leq (1-\beta) \mathbb{E} \left[\|\mathbf{v}_t - \nabla f(\mathbf{x}_t)\|^2 \right] + \frac{2\eta^2 L^2 d}{\beta} + \beta^2 \sigma^2,
 \end{aligned}$$

889 where the third equality is due to the fact $\mathbb{E} [\nabla f(\mathbf{x}_{t+1}; \xi_{t+1}) - \nabla f(\mathbf{x}_{t+1})] = 0$. Summing up, we
 890 can ensure

$$\begin{aligned}
 893 \mathbb{E} \left[\frac{1}{T} \sum_{t=1}^T \|\mathbf{v}_t - \nabla f(\mathbf{x}_t)\|^2 \right] &\leq \frac{\mathbb{E} \left[\|\mathbf{v}_1 - \nabla f(\mathbf{x}_1)\|^2 \right]}{\beta T} + \frac{2\eta^2 L^2 d}{\beta^2} + \beta \sigma^2 \\
 894 &\leq \frac{\sigma^2}{\beta T} + \frac{2\eta^2 L^2 d}{\beta^2} + \beta \sigma^2.
 \end{aligned} \tag{15}$$

900 Incorporating the above into equation (14) and setting that $\beta = \mathcal{O}(T^{-1/2})$, $\eta = \mathcal{O}(d^{-1/2}T^{-3/4})$,
 901 we observe:

$$\begin{aligned}
 905 \mathbb{E} \left[\frac{1}{T} \sum_{t=1}^T \|\nabla f(\mathbf{x}_t)\|_1 \right] &\leq \frac{\Delta_f}{\eta T} + 2\sqrt{d} \cdot \sqrt{\mathbb{E} \left[\frac{1}{T} \sum_{t=1}^T \|\nabla f(\mathbf{x}_t) - \mathbf{v}_t\|^2 \right]} + \frac{\eta L d}{2} \\
 906 &\leq \frac{\Delta_f}{\eta T} + 2\sqrt{d} \cdot \sqrt{\frac{\sigma^2}{\beta T} + \frac{2\eta^2 L^2 d}{\beta^2} + \beta \sigma^2 + \frac{\eta L d}{2}} \\
 907 &= \mathcal{O} \left(\frac{(1 + \Delta_f + \sigma + L) d^{1/2}}{T^{1/4}} \right) \\
 908 &= \mathcal{O} \left(\frac{d^{1/2}}{T^{1/4}} \right),
 \end{aligned}$$

913 which finishes the proof of Theorem 2.
 914
 915

918 C PROOF OF THEOREM 3 AND 4
919920 Since the overall objective function $f(\mathbf{x})$ is L -smooth, we have the following:
921

$$\begin{aligned}
923 \quad f(\mathbf{x}_{t+1}) &\leq f(\mathbf{x}_t) + \langle \nabla f(\mathbf{x}_t), \mathbf{x}_{t+1} - \mathbf{x}_t \rangle + \frac{L}{2} \|\mathbf{x}_{t+1} - \mathbf{x}_t\|^2 \\
924 \\
925 \quad &\leq f(\mathbf{x}_t) - \eta \left\langle \nabla f(\mathbf{x}_t), \text{Sign} \left(\frac{1}{n} \sum_{j=1}^n \mathbf{S}_G(\mathbf{v}_t^j) \right) \right\rangle + \frac{\eta^2 L d}{2} \\
926 \\
927 \quad &= f(\mathbf{x}_t) + \eta \left\langle \nabla f(\mathbf{x}_t), \text{Sign}(\nabla f(\mathbf{x}_t)) - \text{Sign} \left(\frac{1}{n} \sum_{j=1}^n \mathbf{S}_G(\mathbf{v}_t^j) \right) \right\rangle \\
928 \\
929 \quad &\quad - \eta \langle \nabla f(\mathbf{x}_t), \text{Sign}(\nabla f(\mathbf{x}_t)) \rangle + \frac{\eta^2 L d}{2} \\
930 \\
931 \quad &= f(\mathbf{x}_t) + \eta \left\langle \nabla f(\mathbf{x}_t), \text{Sign}(\nabla f(\mathbf{x}_t)) - \text{Sign} \left(\frac{1}{n} \sum_{j=1}^n \mathbf{S}_G(\mathbf{v}_t^j) \right) \right\rangle \\
932 \\
933 \quad &\quad - \eta \|\nabla f(\mathbf{x}_t)\|_1 + \frac{\eta^2 L d}{2} \\
934 \\
935 \quad &\leq f(\mathbf{x}_t) + 2\eta R \sqrt{d} \left\| \frac{\nabla f(\mathbf{x}_t)}{R} - \frac{1}{n} \sum_{j=1}^n \mathbf{S}_G(\mathbf{v}_t^j) \right\| - \eta \|\nabla f(\mathbf{x}_t)\|_1 + \frac{\eta^2 L d}{2}, \\
936 \\
937 \quad &\quad
\end{aligned} \tag{16}$$

942 where the last inequality is because of
943

$$\begin{aligned}
944 \quad &\left\langle \nabla f(\mathbf{x}_t), \text{Sign}(\nabla f(\mathbf{x}_t)) - \text{Sign} \left(\frac{1}{n} \sum_{j=1}^n \mathbf{S}_G(\mathbf{v}_t^j) \right) \right\rangle \\
945 \\
946 \quad &= \sum_{i=1}^d \left\langle [\nabla f(\mathbf{x}_t)]_i, \text{Sign}([\nabla f(\mathbf{x}_t)]_i) - \text{Sign} \left(\left[\frac{1}{n} \sum_{j=1}^n \mathbf{S}_G(\mathbf{v}_t^j) \right]_i \right) \right\rangle \\
947 \\
948 \quad &\leq \sum_{i=1}^d 2 |[\nabla f(\mathbf{x}_t)]_i| \cdot \mathbb{I} \left(\text{Sign}([\nabla f(\mathbf{x}_t)]_i) \neq \text{Sign} \left(\left[\frac{1}{n} \sum_{j=1}^n \mathbf{S}_G(\mathbf{v}_t^j) \right]_i \right) \right) \\
949 \\
950 \quad &\leq \sum_{i=1}^d 2R \left| \frac{[\nabla f(\mathbf{x}_t)]_i}{R} \right| \cdot \mathbb{I} \left(\text{Sign}([\nabla f(\mathbf{x}_t)]_i) \neq \text{Sign} \left(\left[\frac{1}{n} \sum_{j=1}^n \mathbf{S}_G(\mathbf{v}_t^j) \right]_i \right) \right) \\
951 \\
952 \quad &\leq \sum_{i=1}^d 2R \left| \frac{[\nabla f(\mathbf{x}_t)]_i}{R} - \left[\frac{1}{n} \sum_{j=1}^n \mathbf{S}_G(\mathbf{v}_t^j) \right]_i \right| \cdot \mathbb{I} \left(\text{Sign}([\nabla f(\mathbf{x}_t)]_i) \neq \text{Sign} \left(\left[\frac{1}{n} \sum_{j=1}^n \mathbf{S}_G(\mathbf{v}_t^j) \right]_i \right) \right) \\
953 \\
954 \quad &\leq \sum_{i=1}^d 2R \left| \frac{[\nabla f(\mathbf{x}_t)]_i}{R} - \left[\frac{1}{n} \sum_{j=1}^n \mathbf{S}_G(\mathbf{v}_t^j) \right]_i \right| \\
955 \\
956 \quad &= 2R \left\| \frac{\nabla f(\mathbf{x}_t)}{R} - \frac{1}{n} \sum_{j=1}^n \mathbf{S}_G(\mathbf{v}_t^j) \right\|_1 \\
957 \\
958 \quad &\leq 2R \sqrt{d} \left\| \frac{\nabla f(\mathbf{x}_t)}{R} - \frac{1}{n} \sum_{j=1}^n \mathbf{S}_G(\mathbf{v}_t^j) \right\|. \\
959 \\
960 \quad &\quad
\end{aligned} \tag{17}$$

972 Rearranging and taking the expectation over equation (16), we have:
 973

$$\begin{aligned}
 & \mathbb{E}[f(\mathbf{x}_{t+1}) - f(\mathbf{x}_t)] \\
 & \leq 2\eta G\sqrt{d}\mathbb{E}\left[\left\|\frac{\nabla f(\mathbf{x}_t)}{G} - \frac{1}{n}\sum_{j=1}^n S_G(\mathbf{v}_t^j)\right\|\right] - \eta\mathbb{E}[\|\nabla f(\mathbf{x}_t)\|_1] + \frac{\eta^2 Ld}{2} \\
 & \leq 2\eta G\sqrt{d}\mathbb{E}\left[\left\|\frac{\nabla f(\mathbf{x}_t)}{G} - \frac{1}{nG}\sum_{j=1}^n \mathbf{v}_t^j\right\|\right] + 2\eta G\sqrt{d}\mathbb{E}\left[\left\|\frac{1}{n}\sum_{j=1}^n \left(S_G(\mathbf{v}_t^j) - \frac{\mathbf{v}_t^j}{G}\right)\right\|\right] \\
 & \quad - \eta\mathbb{E}[\|\nabla f(\mathbf{x}_t)\|_1] + \frac{\eta^2 Ld}{2} \\
 & \leq 2\eta\sqrt{d}\mathbb{E}\left[\left\|\nabla f(\mathbf{x}_t) - \frac{1}{n}\sum_{j=1}^n \mathbf{v}_t^j\right\|\right] + 2\eta G\sqrt{d}\sqrt{\mathbb{E}\left[\left\|\frac{1}{n}\sum_{j=1}^n \left(S_G(\mathbf{v}_t^j) - \frac{\mathbf{v}_t^j}{G}\right)\right\|^2\right]} \\
 & \quad - \eta\mathbb{E}[\|\nabla f(\mathbf{x}_t)\|_1] + \frac{\eta^2 Ld}{2} \\
 & \leq 2\eta\sqrt{d}\mathbb{E}\left[\left\|\nabla f(\mathbf{x}_t) - \frac{1}{n}\sum_{j=1}^n \mathbf{v}_t^j\right\|\right] + 2\eta G\sqrt{d}\sqrt{\frac{1}{n^2}\sum_{j=1}^n \mathbb{E}\left[\left\|S_G(\mathbf{v}_t^j) - \frac{\mathbf{v}_t^j}{G}\right\|^2\right]} \\
 & \quad - \eta\mathbb{E}[\|\nabla f(\mathbf{x}_t)\|_1] + \frac{\eta^2 Ld}{2} \\
 & \leq 2\eta\sqrt{d}\mathbb{E}\left[\left\|\nabla f(\mathbf{x}_t) - \frac{1}{n}\sum_{j=1}^n \mathbf{v}_t^j\right\|\right] + 2\eta G\sqrt{d}\sqrt{\frac{1}{n^2}\sum_{j=1}^n \mathbb{E}\left[\left\|S_G(\mathbf{v}_t^j)\right\|^2\right]} \\
 & \quad - \eta\mathbb{E}[\|\nabla f(\mathbf{x}_t)\|_1] + \frac{\eta^2 Ld}{2} \\
 & \leq 2\eta\sqrt{d}\mathbb{E}\left[\left\|\nabla f(\mathbf{x}_t) - \frac{1}{n}\sum_{j=1}^n \mathbf{v}_t^j\right\|\right] + \frac{2\eta dG}{\sqrt{n}} - \eta\mathbb{E}[\|\nabla f(\mathbf{x}_t)\|_1] + \frac{\eta^2 Ld}{2}, \tag{18}
 \end{aligned}$$

1007 where the third inequality is due to the fact that $(\mathbb{E}[X])^2 \leq \mathbb{E}[X^2]$, and the forth inequality is
 1008 because of $\mathbb{E}[S_G(\mathbf{v}_t^j)] = \frac{\mathbf{v}_t^j}{G}$, as well as the S_G operation in each node is independent.
 1009

1010 Rearranging the terms and summing up, we have:
 1011

$$\begin{aligned}
 \frac{1}{T}\sum_{i=1}^T \mathbb{E}[\|\nabla f(\mathbf{x}_t)\|_1] & \leq \frac{\Delta_f}{\eta T} + 2\sqrt{d}\mathbb{E}\left[\frac{1}{T}\sum_{i=1}^T \left\|\nabla f(\mathbf{x}_t) - \frac{1}{n}\sum_{j=1}^n \mathbf{v}_t^j\right\|\right] + \frac{2dG}{\sqrt{n}} + \frac{\eta Ld}{2} \\
 & \leq \frac{\Delta_f}{\eta T} + 2\sqrt{d}\sqrt{\mathbb{E}\left[\frac{1}{T}\sum_{i=1}^T \left\|\nabla f(\mathbf{x}_t) - \frac{1}{n}\sum_{j=1}^n \mathbf{v}_t^j\right\|^2\right]} + \frac{2dG}{\sqrt{n}} + \frac{\eta Ld}{2},
 \end{aligned}$$

1020 where the last inequality is due to Jensen's inequality.
 1021

1022 For each worker j , we have the following according to the definition of \mathbf{v}_t^j :
 1023

$$\begin{aligned}
 \mathbf{v}_{t+1}^j - \nabla f_j(\mathbf{x}_{t+1}) & = (1 - \beta) \left(\mathbf{v}_t^j - \nabla f_j(\mathbf{x}_t) \right) + \beta \left(\nabla f_j(\mathbf{x}_{t+1}; \xi_{t+1}^j) - \nabla f_j(\mathbf{x}_{t+1}) \right) \\
 & \quad + (1 - \beta) \left(\nabla f_j(\mathbf{x}_t) - \nabla f_j(\mathbf{x}_{t+1}) \right).
 \end{aligned}$$

1026 Averaging over $\{n\}$ and noting that $\nabla f(\mathbf{x}) = \frac{1}{n} \sum_{j=1}^n \nabla f_j(\mathbf{x})$, we can obtain:
 1027

$$\begin{aligned}
 1028 \quad & \frac{1}{n} \sum_{j=1}^n \mathbf{v}_{t+1}^j - \nabla f(\mathbf{x}_{t+1}) = \frac{1}{n} \sum_{j=1}^n \left(\mathbf{v}_{t+1}^j - \nabla f_j(\mathbf{x}_{t+1}) \right) \\
 1029 \quad & = (1 - \beta) \frac{1}{n} \sum_{j=1}^n \left(\mathbf{v}_t^j - \nabla f_j(\mathbf{x}_t) \right) + \beta \frac{1}{n} \sum_{j=1}^n \left(\nabla f_j(\mathbf{x}_{t+1}; \xi_{t+1}^j) - \nabla f_j(\mathbf{x}_{t+1}) \right) \\
 1030 \quad & + (1 - \beta) \frac{1}{n} \sum_{j=1}^n \left(\nabla f_j(\mathbf{x}_t) - \nabla f_j(\mathbf{x}_{t+1}) \right). \\
 1031 \quad & \\
 1032 \quad & \\
 1033 \quad & \\
 1034 \quad & \\
 1035 \quad & \\
 1036 \quad & \text{Then we have}
 \end{aligned}$$

$$\begin{aligned}
 1037 \quad & \mathbb{E} \left[\left\| \frac{1}{n} \sum_{j=1}^n \mathbf{v}_{t+1}^j - \nabla f(\mathbf{x}_{t+1}) \right\|^2 \right] \\
 1038 \quad & \leq (1 - \beta) \mathbb{E} \left[\left\| \frac{1}{n} \sum_{j=1}^n \left(\mathbf{v}_t^j - \nabla f_j(\mathbf{x}_t) \right) \right\|^2 \right] + \beta^2 \frac{1}{n^2} \sum_{j=1}^n \mathbb{E} \left[\left\| \nabla f_j(\mathbf{x}_{t+1}; \xi_{t+1}^j) - \nabla f_j(\mathbf{x}_{t+1}) \right\|^2 \right] \\
 1039 \quad & + \frac{2}{\beta n} \sum_{j=1}^n \mathbb{E} \left[\left\| \nabla f_j(\mathbf{x}_{t+1}) - \nabla f_j(\mathbf{x}_t) \right\|^2 \right] \\
 1040 \quad & \leq (1 - \beta) \mathbb{E} \left[\left\| \frac{1}{n} \sum_{j=1}^n \left(\mathbf{v}_t^j - \nabla f_j(\mathbf{x}_t) \right) \right\|^2 \right] + \frac{\beta^2 \sigma^2}{n} + \frac{2L^2}{\beta} \|\mathbf{x}_{t+1} - \mathbf{x}_t\|^2 \\
 1041 \quad & \leq (1 - \beta) \mathbb{E} \left[\left\| \frac{1}{n} \sum_{j=1}^n \mathbf{v}_t^j - \nabla f(\mathbf{x}_t) \right\|^2 \right] + \frac{\beta^2 \sigma^2}{n} + \frac{2L^2 \eta^2 d}{\beta}.
 \end{aligned}$$

1055 By summing up and rearranging, we observe

$$\begin{aligned}
 1056 \quad & \mathbb{E} \left[\frac{1}{T} \sum_{t=1}^T \left\| \frac{1}{n} \sum_{j=1}^n \mathbf{v}_t^j - \nabla f(\mathbf{x}_t) \right\|^2 \right] \leq \frac{\mathbb{E} \left[\left\| \frac{1}{n} \sum_{j=1}^n \mathbf{v}_1^j - \nabla f(\mathbf{x}_1) \right\|^2 \right]}{\beta T} + \frac{\beta \sigma^2}{n} + \frac{2L^2 \eta^2 d}{\beta^2} \\
 1057 \quad & \leq \frac{\sigma^2}{n \beta T} + \frac{\sigma^2 \beta}{n} + \frac{2L^2 \eta^2 d}{\beta^2}.
 \end{aligned} \tag{19}$$

1064 Finally, we can ensure that

$$\begin{aligned}
 1065 \quad & \frac{1}{T} \sum_{i=1}^T \|\nabla f(\mathbf{x}_t)\|_1 \leq \frac{\Delta_f}{\eta T} + \frac{2dG}{\sqrt{n}} + \frac{\eta Ld}{2} + 2\sqrt{d} \sqrt{\mathbb{E} \left[\frac{1}{T} \sum_{i=1}^T \left\| \nabla f(\mathbf{x}_t) - \frac{1}{n} \sum_{j=1}^n \mathbf{v}_t^j \right\|^2 \right]} \\
 1066 \quad & \leq \frac{\Delta_f}{\eta T} + \frac{2dG}{\sqrt{n}} + \frac{\eta Ld}{2} + 2\sqrt{d} \sqrt{\frac{\sigma^2}{n \beta T} + \frac{\sigma^2 \beta}{n} + \frac{2L^2 \eta^2 d}{\beta^2}}.
 \end{aligned}$$

1072 By setting $\beta = \frac{1}{2}$ and $\eta = \mathcal{O}(T^{-1/2} d^{-1/2})$, we have

$$\frac{1}{T} \sum_{i=1}^T \|\nabla f(\mathbf{x}_t)\|_1 = \mathcal{O} \left(\frac{d^{1/2}}{T^{1/2}} + \frac{d}{n^{1/2}} \right).$$

1077 By setting $\beta = \frac{1}{2}$ and $\eta = \mathcal{O}(n^{-1/2})$, we have

$$\frac{1}{T} \sum_{i=1}^T \|\nabla f(\mathbf{x}_t)\|_1 = \mathcal{O} \left(\frac{n^{1/2}}{T} + \frac{d}{n^{1/2}} \right).$$

1080 **D PROOF OF THEOREM 5**
10811082 Due to the fact that the overall objective function $f(\mathbf{x})$ is L -smooth, we have the following:
1083

1084
$$f(\mathbf{x}_{t+1}) \leq f(\mathbf{x}_t) + \langle \nabla f(\mathbf{x}_t), \mathbf{x}_{t+1} - \mathbf{x}_t \rangle + \frac{L}{2} \|\mathbf{x}_{t+1} - \mathbf{x}_t\|^2$$

1085
$$\leq f(\mathbf{x}_t) - \eta \left\langle \nabla f(\mathbf{x}_t), \mathbf{S}_1 \left(\frac{1}{n} \sum_{j=1}^n \mathbf{S}_G(\mathbf{v}_t^j) \right) \right\rangle + \frac{\eta^2 L d}{2}$$

1086
$$= f(\mathbf{x}_t) + \eta \left\langle \nabla f(\mathbf{x}_t), \frac{\nabla f(\mathbf{x}_t)}{G} - \mathbf{S}_1 \left(\frac{1}{n} \sum_{j=1}^n \mathbf{S}_G(\mathbf{v}_t^j) \right) \right\rangle$$

1087
$$- \eta \left\langle \nabla f(\mathbf{x}_t), \frac{\nabla f(\mathbf{x}_t)}{G} \right\rangle + \frac{\eta^2 L d}{2}$$

1088
$$= f(\mathbf{x}_t) + \eta \left\langle \nabla f(\mathbf{x}_t), \frac{\nabla f(\mathbf{x}_t)}{G} - \mathbf{S}_1 \left(\frac{1}{n} \sum_{j=1}^n \mathbf{S}_G(\mathbf{v}_t^j) \right) \right\rangle - \frac{\eta}{G} \|\nabla f(\mathbf{x}_t)\|^2 + \frac{\eta^2 L d}{2}.$$

1089

1090 Taking expectations leads to:
1091

1092
$$\mathbb{E}[f(\mathbf{x}_{t+1}) - f(\mathbf{x}_t)]$$

1093
$$\leq \eta \mathbb{E} \left[\left\langle \nabla f(\mathbf{x}_t), \frac{1}{G} \nabla f(\mathbf{x}_t) - \mathbf{S}_1 \left(\frac{1}{n} \sum_{j=1}^n \mathbf{S}_G(\mathbf{v}_t^j) \right) \right\rangle \right] - \frac{\eta}{G} \mathbb{E} [\|\nabla f(\mathbf{x}_t)\|^2] + \frac{\eta^2 L d}{2}$$

1094
$$= \eta \mathbb{E} \left[\left\langle \nabla f(\mathbf{x}_t), \frac{1}{G} \nabla f(\mathbf{x}_t) - \frac{1}{n} \sum_{j=1}^n \mathbf{S}_G(\mathbf{v}_t^j) \right\rangle \right] - \frac{\eta}{G} \mathbb{E} [\|\nabla f(\mathbf{x}_t)\|^2] + \frac{\eta^2 L d}{2}$$

1095
$$= \eta \mathbb{E} \left[\left\langle \nabla f(\mathbf{x}_t), \frac{1}{G} \nabla f(\mathbf{x}_t) - \frac{1}{nG} \sum_{j=1}^n \mathbf{v}_t^j \right\rangle \right] - \frac{\eta}{G} \mathbb{E} [\|\nabla f(\mathbf{x}_t)\|^2] + \frac{\eta^2 L d}{2} \quad (20)$$

1096
$$\leq \eta \mathbb{E} \left[\frac{1}{2G} \|\nabla f(\mathbf{x}_t)\|^2 + \frac{1}{2G} \left\| \nabla f(\mathbf{x}_t) - \frac{1}{n} \sum_{j=1}^n \mathbf{v}_t^j \right\|^2 \right] - \frac{\eta}{G} \mathbb{E} [\|\nabla f(\mathbf{x}_t)\|^2] + \frac{\eta^2 L d}{2}$$

1097
$$= \frac{\eta}{2G} \mathbb{E} \left[\left\| \nabla f(\mathbf{x}_t) - \frac{1}{n} \sum_{j=1}^n \mathbf{v}_t^j \right\|^2 \right] - \frac{\eta}{2G} \mathbb{E} [\|\nabla f(\mathbf{x}_t)\|^2] + \frac{\eta^2 L d}{2}.$$

1098

1099 Rearranging the terms and summing up:
1100

1101
$$\frac{1}{T} \sum_{i=1}^T \mathbb{E} [\|\nabla f(\mathbf{x}_t)\|^2] \leq \frac{2\Delta_f G}{\eta T} + \mathbb{E} \left[\frac{1}{T} \sum_{i=1}^T \left\| \nabla f(\mathbf{x}_t) - \frac{1}{n} \sum_{j=1}^n \mathbf{v}_t^j \right\|^2 \right] + \eta L d G$$

1102
$$\leq \frac{2\Delta_f G}{\eta T} + \mathbb{E} \left[\frac{1}{n} \sum_{j=1}^n \frac{1}{T} \sum_{i=1}^T \left\| \nabla f_j(\mathbf{x}_t) - \mathbf{v}_t^j \right\|^2 \right] + \eta L d G.$$

1103

1104 For each worker j , according to the definition of \mathbf{v}_t^j , we have:
1105

1106
$$\mathbf{v}_{t+1}^j - \nabla f_j(\mathbf{x}_{t+1}) = (1 - \beta) \left(\mathbf{v}_t^j - \nabla f_j(\mathbf{x}_t) \right) + \beta \left(\nabla f_j(\mathbf{x}_{t+1}; \xi_{t+1}^j) - \nabla f_j(\mathbf{x}_{t+1}) \right)$$

1107
$$+ (1 - \beta) (\nabla f_j(\mathbf{x}_t) - \nabla f_j(\mathbf{x}_{t+1})).$$

1108

Table 5: Optimal hyperparameters for fine-tuning GPT-2 on Alpaca.

Method	SGDM	signSGD	EF-signSGD	AdamW	Signum
lr	1e-1	1e-4	1e-0	5e-4	1e-4
β_1	0.9	–	–	0.9	0.75
β_2	–	–	–	0.95	–

Table 6: Optimal hyperparameters for fine-tuning Qwen3-0.6B on Alpaca.

Method	SGDM	signSGD	EF-signSGD	AdamW	Signum
lr	5e-2	1e-5	5e-1	5e-5	1e-5
β_1	0.9	–	–	0.9	0.75
β_2	–	–	–	0.95	–

Then we have

$$\begin{aligned}
& \mathbb{E} \left[\left\| \mathbf{v}_{t+1}^j - \nabla f_j(\mathbf{x}_{t+1}) \right\|^2 \right] \\
& \leq (1 - \beta) \mathbb{E} \left[\left\| \mathbf{v}_t^j - \nabla f_j(\mathbf{x}_t) \right\|^2 \right] + \beta^2 \mathbb{E} \left[\left\| \nabla f_j(\mathbf{x}_{t+1}; \xi_{t+1}^j) - \nabla f_j(\mathbf{x}_{t+1}) \right\|^2 \right] \\
& \quad + \frac{2}{\beta} \mathbb{E} \left[\left\| \nabla f_j(\mathbf{x}_{t+1}) - \nabla f_j(\mathbf{x}_t) \right\|^2 \right] \\
& \leq (1 - \beta) \mathbb{E} \left[\left\| \mathbf{v}_t^j - \nabla f_j(\mathbf{x}_t) \right\|^2 \right] + \beta^2 \sigma^2 + \frac{2L^2}{\beta} \|\mathbf{x}_{t+1} - \mathbf{x}_t\|^2 \\
& \leq (1 - \beta) \mathbb{E} \left[\left\| \mathbf{v}_t^j - \nabla f_j(\mathbf{x}_t) \right\|^2 \right] + \beta^2 \sigma^2 + \frac{2L^2 \eta^2 d}{\beta}.
\end{aligned}$$

As a result, we know that

$$\mathbb{E} \left[\frac{1}{n} \sum_{j=1}^n \frac{1}{T} \sum_{t=1}^T \left\| \mathbf{v}_t^j - \nabla f_j(\mathbf{x}_t) \right\|^2 \right] \leq \frac{\sigma^2}{\beta T} + \sigma^2 \beta + \frac{2L^2 \eta^2 d}{\beta^2}.$$

Finally, we can obtain the final bound:

$$\begin{aligned}
\mathbb{E} \left[\frac{1}{T} \sum_{i=1}^T \left\| \nabla f(\mathbf{x}_t) \right\| \right] & \leq \sqrt{\mathbb{E} \left[\frac{1}{T} \sum_{i=1}^T \left\| \nabla f(\mathbf{x}_t) \right\|^2 \right]} \\
& \leq \sqrt{\frac{2\Delta_f G}{\eta T} + \eta L d G + \frac{\sigma^2}{\beta T} + \sigma^2 \beta + \frac{2L^2 \eta^2 d}{\beta^2}}.
\end{aligned}$$

That is to say, by setting $\beta = \eta^{2/3} d^{1/3}$, $\eta = \mathcal{O}(\min\{\frac{1}{T^{1/2} d^{1/2}}, \frac{1}{T^{3/5} d^{1/5}}\})$, we can obtain the convergence rate of $\mathcal{O}(\max\{\frac{d^{1/4}}{T^{1/4}}, \frac{d^{1/10}}{T^{1/5}}\})$.

E EXPERIMENTAL DETAILS

In this section, we present the omitted details in our experiments.

E.1 OPTIMAL HYPERPARAMETERS

The tuned learning rates and β_1, β_2 coefficients for all methods are shown in Tables 5 and 6, which can be used to reproduce the results in Table 4. We underline that our tuned optimal learning rate of

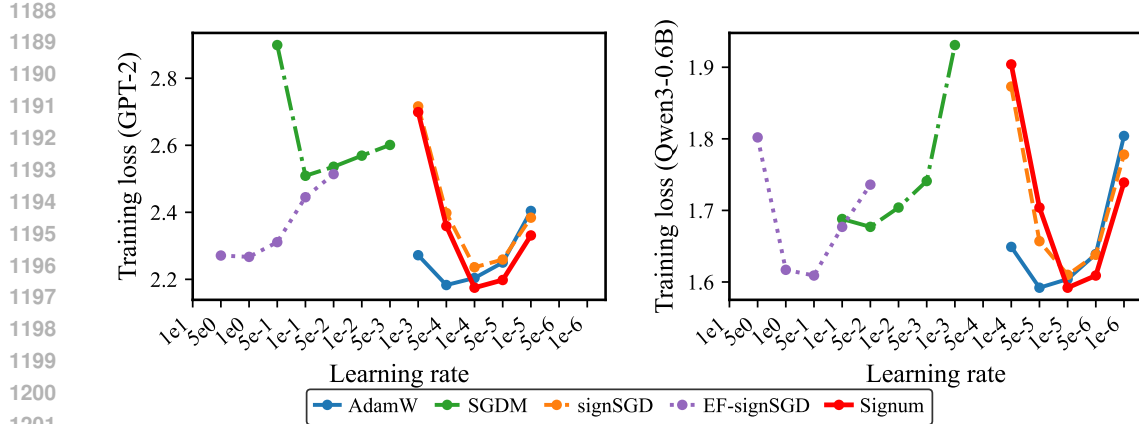


Figure 3: Sensitivity result across different learning rates.

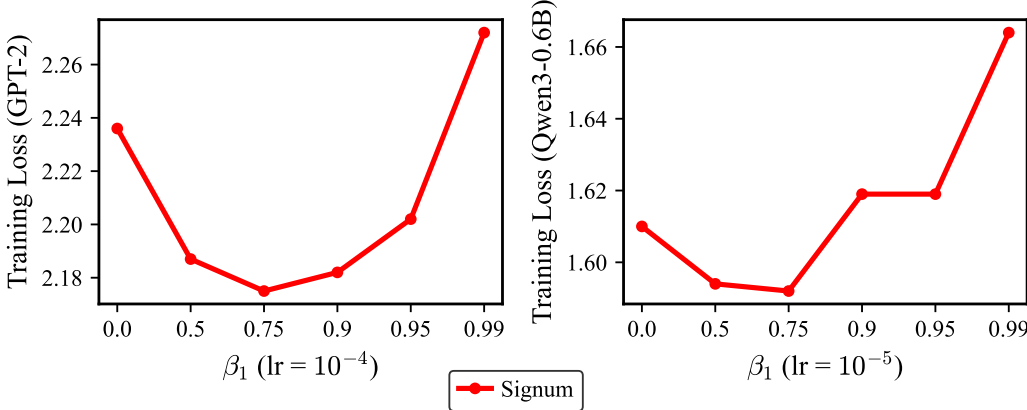


Figure 4: Sensitivity result across different momentum coefficients.

AdamW is **5 times** that of Signum, which aligns perfectly well with the theoretical value (Kosson et al., 2024), as well as the recent empirical discovery (Liu et al., 2025a)¹.

E.2 SENSITIVITY ANALYSIS

Then, we conduct a sensitivity analysis across different learning rates and different momentum coefficients β_1 (representing $1 - \beta$ in Algorithm 1). We keep the other hyperparameters fixed to their optimal values and vary only the learning rate or the momentum coefficient to see the changes in training loss values. Figure 3 shows the training losses on GPT-2 and Qwen3-0.6B for all methods across a wide range of learning rates. Our method remains valid and stable within a certain range. While we observe that AdamW is less sensitive to learning rate changes, this is largely due to its smaller update RMS norm (Liu et al., 2025a). We also investigate the sensitivity of β_1 in Signum, as shown in Figure 4. The results demonstrate that Signum remains quite robust to different momentum coefficients.

¹Such phenomenon stems from the idea of matching update RMS norms between sign-based methods and AdamW (Liu et al., 2025a). Signum has an inherent update RMS norm of 1, while the value of AdamW typically ranges from 0.2 to 0.4 (Liu et al., 2025a;b) with theoretical estimation of $\sqrt{(1 - \beta_1)/(1 + \beta_1)}$ (Kosson et al., 2024). Matching these terms (1 VS 0.2) gives a rough law of $1r_{\text{AdamW}} \approx 51r_{\text{Signum}}$.

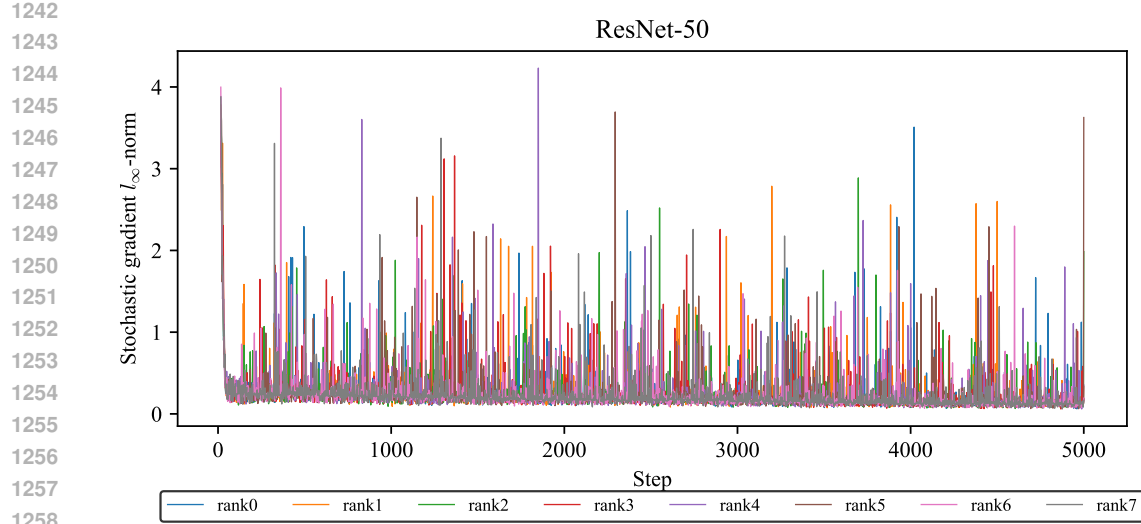


Figure 5: Stochastic gradient trajectory on the CIFAR-100 dataset.

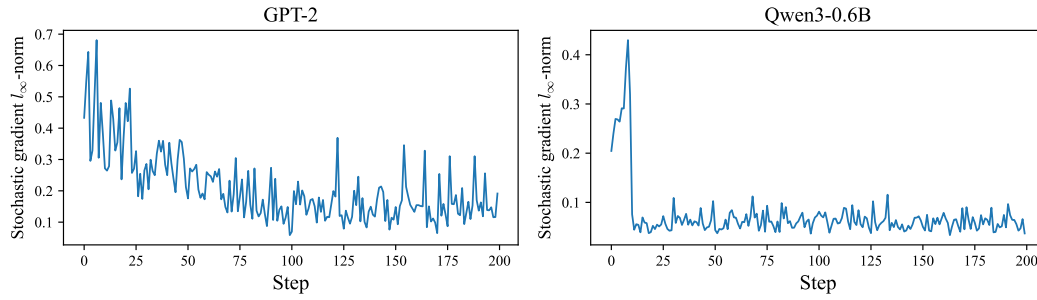


Figure 6: Stochastic gradient trajectory on the Alpaca dataset.

E.3 EMPIRICAL VALIDATION OF BOUNDED STOCHASTIC GRADIENTS

We investigate the infinity norm of stochastic gradients along the training trajectory. The direct evidence in Figure 5 shows that Assumption 8 is well-satisfied in distributed environments. We also consider the centralized environment (where the number of nodes $n = 1$), whose trend is depicted in Figure 6. It is evident that the stochastic gradients are bounded in both scenarios, highlighting the rationality of Assumption 8.